GALILEAN MOON TOUR USING SIMPLIFIED TRAJECTORY COMPUTATIONAL TECHNIQUES

A Thesis presented to the Faculty of the Graduate School

University of Missouri-Columbia

In Partial Fulfillment

Of the Requirements for the Degree

Master of Science

---

by

RYAN WILLIAMS

Dr. Craig Kluever, Thesis Supervisor

MAY 2006

The undersigned, appointed by the Dean of the Graduate School,

have examined the thesis entitled

GALILEAN MOON TOUR USING SIMPLIFIED TRAJECTORY COMPUTATIONAL TECHNIQUES

Presented by Ryan Williams

A candidate for the degree of Master of Science

And herby certify that in their opinion it is worthy of acceptance

---

Dr. Craig Kluever

Dr. Roger Fales

Dr. Cerry Klein

Acknowledgements

Graduate school was an excellent decision for me to attend. Graduate school has helped me further educate myself in the areas I am truly interested in. Graduate school helped me learn how to work on a large project and it taught me to do adequate amounts of research.

I would like to thank my thesis advisor Dr. Craig Kluever for working with me over the past two years. Dr. Kluever has taught me in many classes as well, and his expertise in the area of mechanical and aerospace engineering, along with passion for helping students learn has been very helpful in working with him.

I would like to thank Dr. Roger Fales for teaching me for a few years, as well as being a member on my thesis committee.

I would like to thank Dr. Cerry Klein for being on my thesis committee.

I would like to thank Yang Gao, a PhD student of Dr. Kluever's, for helping teach me, and being patient with my learning process of both the FORTRAN language, as well as the DTOM program.

I would like to thank Michael Martini and the rest of the employees of NASA Glenn Research Center for teaching me to run SNAP and helping me set it up on my computer.

Lastly I would like to thank my family. My mother, Mary Williams, my father, Chris Williams, and my sisters, Amy and Jessica Williams, have always helped me and supported me with every decision of my life. Without their support I could not have accomplished anything.

Table of Contents

LIST OF FIGURES

LIST OF TABLES

LIST OF NONMENCLATURE

a	=	semimajor axis, km
a_T	=	acceleration due to thrust
c	=	exhaust velocity, m/s
C	=	Jacobi's constant, km^2/s^2
E	=	energy, km^2/s^2
f	=	force, N
F	=	gravitational force, kN
g	=	Earth's gravitational constant, km/s^2
G	=	universal gravitational constant, m^3/kgs^2
H	=	angular momentum, km^3/s^2
i	=	inclination, deg
I_{sp}	=	specific impulse, s
K	=	vehicle parameter constant
L1	=	libration point, km
m	=	mass, kg
$\dot{m}$	=	mass flow rate, kg/s
n	=	line of nodes
p	=	semilatus rectum, km
P	=	power, kW
r	=	radius, km
$\ddot{r}$	=	acceleration, km/s^2
T	=	thrust, N

T/W = thrust to weight

u = unit vector

V = velocity, km/s

α = steering angle, deg

ε = eccentricity

ΔV = propulsive effort, km/s

μ = planet's gravitational parameter, km^3/s^2

Φ = flight path angle, deg

ρ = distance to spacecraft, km

η = efficiency

π = constant pi

ξ = rotating unit vector in x direction

Ω = right ascension of the ascending node, deg

υ = true anomaly, deg

ω = argument of periapsis, deg

ζ = rotating unit vector in y direction

Subscripts

a = apoapsis

f = final

i = initial

L1 = combination of the gravitational parameters of the planet and the moon

m = moon

n = normal dircetion

p = periapsis

pl = planet

pp = power system

r = radial direction

rel = relative to coordinate plane

rs = radiation shielding

sc = spacecraft

SOI = sphere of influence

st = structure

t = tanks

θ = along track direction

CHAPTER 1 INTRODUCTION

Problem Overview

Interplanetary space travel has played an important role in the development of our knowledge of the solar system. For years scientists have been sending probes into the farthest reaches of the solar system to explore the unknown. While some planetary targets are relatively easily attainable, others pose a somewhat difficult time reaching them in a timely and efficient manner. The Jovian system, Jupiter and its moons, is not difficult to reach, however because of Jupiter's massive gravity pull on a spacecraft; it takes a somewhat delicate approach to design a trajectory in which a tour of the moons can occur. It is desired to find the mass and time necessary for a spacecraft to take a tour of the four largest Galilean moons: Io, Europa, Ganymede, and Callisto. In order for enough data to be collected by the probes on the spacecraft, the spacecraft must enter a low orbit about each of the moons individually before continuing on with the trip.

The primary design variable that must be addressed is how the spacecraft is propelled. There are currently two main methods of propulsion for spacecrafts: chemical propulsion which is very high thrust but low efficiency, and electric propulsion which is very low thrust, however it yields much better efficiency. As expected, the time of travel between electric propulsion and chemical propulsion can differ greatly, with chemical having a much shorter trip time on average. Another primary difference between chemical and electric propulsion is that chemical propulsion occurs in one large, nearly

impulsive, short burn followed by a long coasting stage, while electric propulsion can be "firing" its engines for the majority of the trip.

Literature Overview

Celestial Mechanics

The first concept that must be understood is celestial dynamics. Celestial dynamics describes the motion of the trajectory of a spacecraft. There are two types of orbits that a spacecraft can follow: captured trajectory around a body (ellipse, circle), or an escaping trajectory from a body (parabola, hyperbola). Figure 1.1 shows the four possible trajectories that a spacecraft can have [1].

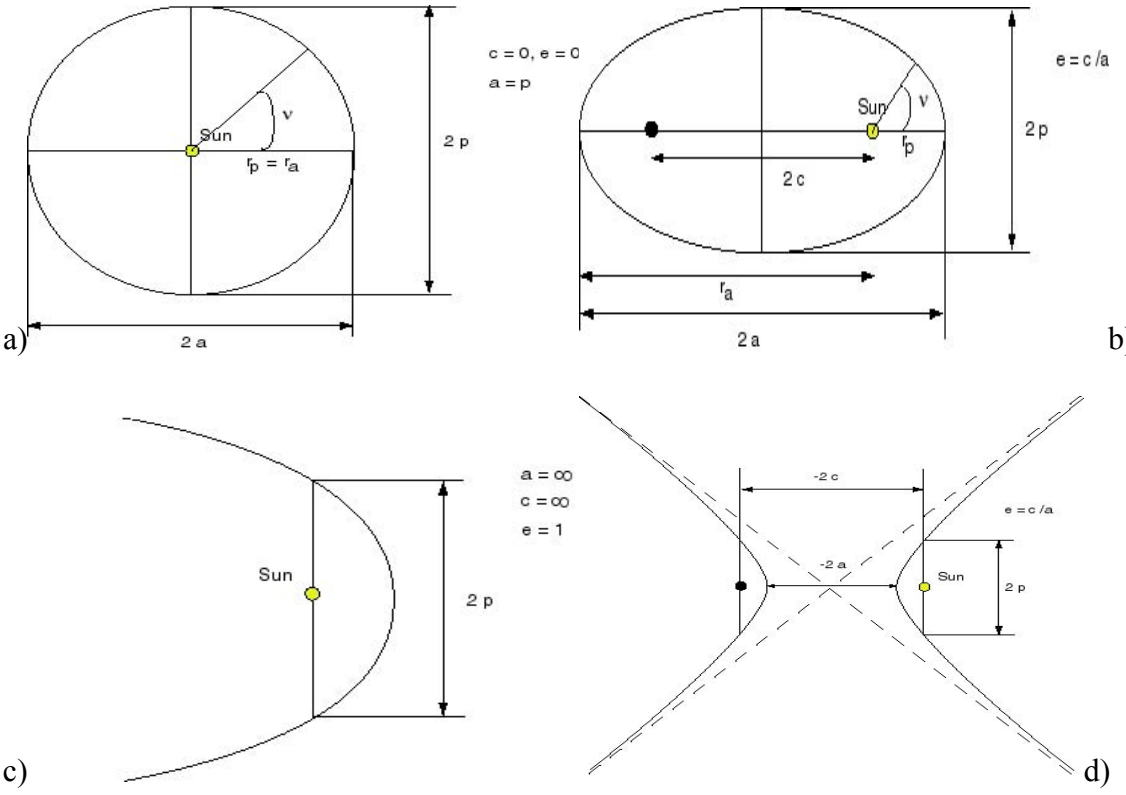

Fig. 1.1. *The four types of trajectories of a spacecraft, a) circle, b) ellipse, c) parabola, d) hyperbola.*

No matter what type of trajectory a spacecraft is in, there are six orbital elements that can pinpoint the location of the spacecraft: 1) a, semimajor axis, 2) ε, eccentricity, 3) i, inclination, 4) ω, argument of periapsis, 5) Ω, right ascension of the ascending node, 6) υ, true anomaly. The semimajor axis and eccentricity determine the size and shape of the orbit respectively. The true anomaly gives the location of the spacecraft in the orbit. Figure 1.1 shows how the semimajor axis and eccentricity affect the shape of an orbit, as well as where the spacecraft is located in the orbit via the true anomaly. The inclination, argument of periapsis, and right ascension of the ascending node give the three-dimensional orientation of the orbit in space. Figure 1.2 shows how each of the aligning elements affects the orbit where **z** is the zenith and **n** is the line of nodes [2].

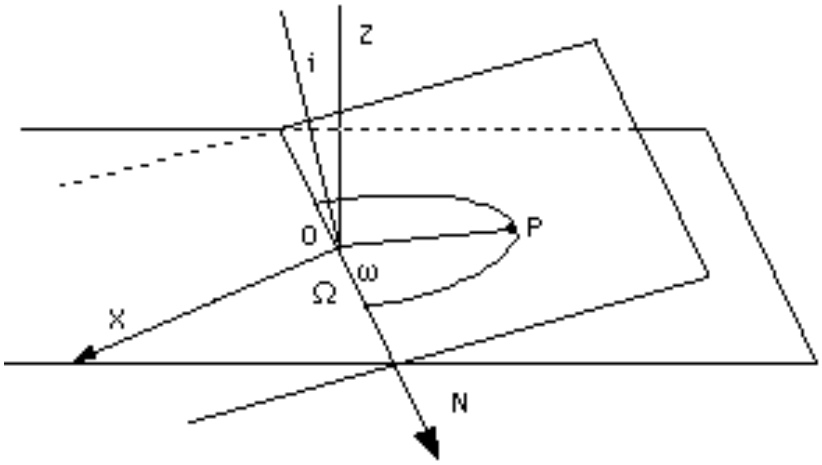

Fig. 1.2. The *orientation of an orbit in three dimensional space*.

Jovian System

Jupiter is the largest planet in the solar system with an equatorial radius of 71,492 km. It is also the most massive planet containing a mass of 1.9×10^{27} kg, more mass than all of the other planets in the solar system combined. Jupiter is the fifth planet from the sun with a semimajor axis of 778,330,000 km. A year on Jupiter is much longer than a year on Earth, as a year is 4333 Earth days long. Jupiter's orbit about the Sun is nearly a planar circle having an eccentricity of 0.048 and an inclination of a mere 1.3 deg. Jupiter also has four rings: Halo, Main, Inner Gossamer, and Outer Gossamer. These rings are invisible from Earth, however were discovered on the Voyager 1 mission in 1979 [3]. Jupiter also has a large, intense magnetic field. Jupiter's magnetic field is over ten times as strong as that of Earth's own Van Allen radiation belts. The radiation belt extends out over a million and a half kilometers. Jupiter has sixty-one known satellites; however four of the satellites are much larger than the rest. The four satellites are Jupiter's four largest moons: Io, Europa, Ganymede, and Callisto. Galileo discovered these moons in the year 1610 with nothing more than a home telescope, which is why these four moons are referred to as the Galilean satellites. Table 1.1 gives all the orbital information for the Galilean moons [4].

Table 1.1. *Orbital data for the Galilean moons.*

Moon	Mass (10^{22}kg)	Radius (km)	a (10^{5}km)	e	inc (deg)	period (days)
Io	8.94	1815	4.216	0.004	0.04	1.78
Europa	4.8	1569	6.709	0.009	0.47	3.55
Ganymede	14.8	2631	10.7	0.002	0.19	7.15
Callisto	10.8	2400	18.83	0.007	0.28	16.7

Io is the Galilean satellite closest to Jupiter with a semimajor axis of 421,600 km. Io is the most volcanic body known in the solar system. Its surface is primarily made up of volcanoes, lava flows, and lava lakes. Io's surface is slowly being swept away by Jupiter's magnetosphere. Io is the second least massive moon with a mass of 8.94×10^{22} kg. Io has an equatorial radius of 1,815 km. Io's orbit is almost planar with an inclination of only 0.4 deg, and is basically circular with an eccentricity of 0.004. The orbital period of Io is only 1.78 days [4].

Europa is the second closest Galilean satellite to Jupiter with a semimajor axis of 670,900 km. Europa's surface is one of the brightest in the solar system, which is because of the icy crust on its surface. Europa is also the smoothest of Jupiter's moons because it lacks the large raters that characterize the other moons. Europa is believed to possibly be internally active, this stems from the discovery that its crust may have, or have had in the past, liquid water on or below its surface that could harbor life. Futhermore Europa has an oxygen atmosphere. The possibility of life is a main reason that scientists want to further investigate Europa. Europa is the least massive moon and has a mass of 4.8×10^{22} kg. It has an equatorial radius of 1,569 km. Europa's orbit is also

nearly planar and circular with and inclination of 0.47 deg and an eccentricity of 0.009. Europa's period is 3.55 days [4].

Ganymede is the next closest Galilean moon to Jupiter with a semimajor axis of 1,070,000 km. Ganymede has both light and dark regions, the light regions being comprised of icy surfaces similar to that of Europa, and the dark regions being mountainous with volcanoes and lava flows. Scientists believe that Ganymede has a thin oxygen atmosphere like Europa's but not as prevalent. Ganymede is the largest of the Galilean moons, as well as the largest moon in the solar system. It is twice as large as Pluto, and it is also larger than Mercury. Ganymede has a mass of 1.48×10^{23} kg. Ganymede's equatorial radius is 2,631 km which is 41 percent the size of Earth. Ganymede's orbit is similar to that of the other Galilean moons being virtually planar and circular with and inclination of 0.19 deg and an eccentricity of 0.002. The orbital period of Ganymede is 7.15 days [4].

Callisto is the Galilean moon furthest from Jupiter. Its semimajor axis is 1,883,000 km. Callisto is the only Galilean moon that orbits outside of Jupiter's main radiation belt. Callisto does not have any large mountains; however it does have two very large craters caused by meteor impacts. These impacts punctured Callisto's crust causing water to spread over the surface of the moon. Callisto has saltwater oceans beneath its crust; however it lacks any form of atmosphere. Callisto is the second biggest Galilean moon, and the third biggest moon in the solar system. It is about the size of Mercury. Callisto has a mass of 1.08×10^{23} kg, and an equatorial radius of 2,440 km. Like all of the Galilean moons, Callisto's orbit is practically planar and circular with an

inclination of 0.28 deg and eccentricity of 0.007. Callisto's orbital period is 16.7 days [4].

Jupiter Moon Tours

There has been one primary mission that has been launched that orbited Jupiter, the Galileo mission. The Galileo mission used chemical propulsion and five gravity assists: Venus, Earth, the asteroid Gaspra, Earth, and the asteroid Ida in order to reach Jupiter [5]. The Galileo mission had several firsts for spacecrafts: first mission to make a close flyby of an asteroid (Gaspra), first mission to discover a spacecraft of an asteroid (Ida's spacecraft Dactyl), first multispectral study of the Moon, first atmospheric probe to enter Jupiter's atmosphere, first spacecraft to go into orbit around Jupiter, and the first direct observations of a comet impacting a planet (Shoemaker-Levy 9) [6]. Along with these firsts, the Galileo spacecraft was sent to examine the physical properties of the moons. The Galileo spacecraft never captured into an orbit about any of the moons however, it only did flybys of each of the moons in its orbit about Jupiter.

Another mission that has been discussed will have a spacecraft actually orbit Jupiter's moons. This tour is called JIMO (Jupiter Icy Moons Orbiter). The Jet Propulsion Laboratory (JPL) has done all the calculations for this mission. The first step in calculating JIMO's trajectory is deciding what type of power to use. Sims shows that it is necessary to use highly efficient nuclear electric propulsion if low-thrust is to be used in the JIMO mission [7]. Nuclear electric propulsion uses a nuclear reactor to power the spacecraft. Electric propulsion thrusters have a few properties that affect the thrust of the

engine as well as the amount of fuel mass that is consumed: specific impulse, mass flow rate, power, and thrust. The power of an engine is found by the size of the reactor. Therefore, given a specific reactor, or assuming an engine with constant power, as the specific impulse of the engine increases the mass flow rate for the fuel decreases, however the thrust also decreases. However, the higher the specific impulse an engine has the better efficiency the engine has. This gives a trade off between efficiency and thrust. Whiffen then discusses the necessity to have both high specific impulse ion thrusters which have better efficiency but create less thrust, as well as low specific impulse Hall thrusters which create more thrust but have worse efficiency in order to have more power when necessary and more efficiency at the other times [8].

Once the type of propulsion has been decided, finding proper injection conditions is the next step. Kowalkowski found that using a low-thrust propulsion system allows the interplanetary trajectory performance to be insensitive to variations to injection conditions due to the long injection period and consecutive orbits with favorable geometry [9]. Once the spacecraft has reached Jupiter's sphere of influence, the next step is to find the best order in which the moons should be visited. Whiffen found that the best order in which to visit the moons is by starting at the outermost moon, Callisto, and working inward. The reason for choosing this order is actually not performance but rather the total integrated radiation dosage that the spacecraft receives [8].

Once the order that the moons will be visited has been chosen, the trajectories to capture into each moon must be discussed. Before capturing into Callisto the spacecraft does three Callisto flybys to decrease the energy of the orbit. The flybys have a

resonance of 1:7, 1:3, and 3:4 [8]. The resonance of two bodies is the ratio of the number of times each bodies completes an entire orbital revolution. Once all of the flybys have occurred, simply using low-thrust propulsion can capture the spacecraft into an orbit about Callisto. With low thrust engines capturing into a body requires that the spacecraft complete many spirals about the body slowly decreasing the energy of the orbit.

In the transfer from Callisto to Ganymede there are flybys of both Callisto and Ganymede in order to reduce the energy. There are two different resonances that can be chosen between for this leg of the trajectory: a 4:3 or 5:4 Callisto resonance. The item to optimize in transferring from Callisto to Ganymede is minimum fuel. The spiral into Ganymede is analogous to the capture into Callisto. There are flybys to lower the energy, followed by low-thrust to capture the spacecraft into Ganymede.

Unlike in the transfer from Callisto to Ganymede, the transfer from Ganymede to Europa requires minimizing the time of flight. The most rapid trajectory possible is needed due to the high levels of radiation that the spacecraft undergoes when within Jupiter's main radiation belt. The Ganymede to Europa transfer is the first portion of the trajectory in which the lower efficiency higher powered thrusters are used to minimize the flight time. The resonances for this trajectory are 4:3 for Ganymede and 3:4 for Europa [10]. The outer orbits in the capture into Europa are very chaotic, however when the spacecraft passes the Europa-Jupiter Lagrange point, the point at which Europa's gravitational pull is greater than Jupiter's gravitational pull on the spacecraft, the orbits begin to become elliptical [11]. The spacecraft remains in Europa's orbit until the

radiation overcomes the system. In order for the spacecraft to remain in the orbit for the longest period of time, the spacecraft should be in a polar orbit [12,13].

Problem Statement and Solution Overview

Nuclear electric propulsion is the type of engine thruster that will find best results for completing a Galilean moon tour. The amount of time and fuel mass necessary to do a complete tour of the Galilean moons with nuclear electric propulsion will be discussed. When JPL calculated the trajectory for the JIMO mission, an incredibly computer intensive and extremely sensitive method was used. These conditions required a large amount of computational time as well as very exact initial conditions [8]. JPL's method could take up to two weeks to compute an exact trajectory. Our goal is to find a simplified analysis in which computationally fast and efficient solution approximations can be found in minutes.

It will be assumed that the spacecraft has successfully made the transfer from Earth to the Jovian system and has just entered Jupiter's sphere of influence, or gravity field, in a parabolic orbit, an orbit where eccentricity equals one. Our method removes the injection necessary to get the spacecraft from Earth to Jupiter; which is being ignored due to the fact that the trajectory from Earth to Jupiter is assumed to be done with a launch vehicle. From these initial conditions, the time and mass of fuel necessary to transfer to, as well as capture into and escape from, each of the Galilean moons will be

found. The spacecraft in our study will only have one type of low-thrust engine unlike the JIMO trajectory in order to simplify the problem.

The trajectory will be broken down into segments: transferring to the first moon, transferring between moons, capturing into each moon, and escaping from each moon. In the transfer to the first moon section, an orbital averaging technique will be used in order to reduce the computational time to calculate the revolutions. In the transferring between moons section, an analytic method will be used to solve for the variables because of the very high numbers of revolutions about Jupiter necessary to complete the transfer. In both of the trajectories involving the moons, the same analytic method will be used to calculate the mass and time out to a cutoff point, where an n-body integrator will take over and calculate the variables to escape. Once each of the legs of the trajectory has been computed, they will be added together to find the final result. The final mass and total trip time can easily be found when given the initial conditions of the thruster's parameters.

CHAPTER 2 SYSTEM DYNAMICS AND SIMULATION

Celestial Mechanics

Two-Body Problem

The first concept to be discussed is celestial dynamics. Celestial dynamics is based on *Newton's law of universal gravitation* which states*, two bodies will exert a force on each other that acts along the line joining the bodies and that is directly proportional to the product of their masses and inversely proportional to the square of the distance between them* [14]. Considering each body as a homogeneous sphere, the force exerted between two bodies having masses m_1 and m_2 can now be found using the gravitational constant, G, and Newton's law, and is given in Eq. (2.1)

$$F = \frac{Gm_1m_2}{r^2} \tag{2.1}$$

The forces that celestial bodies apply to each other are what make the planets in the solar system revolve around the sun. Each body applies a force to every other body in the solar system; however the magnitude of the force applied differs greatly between bodies due to their distance apart as well as their mass. When examining the trajectory of a spacecraft in interplanetary travel, assuming the spacecraft is purely in a two-body system with the sun is a decent approximation due to the magnitude of the force that the sun applies to the spacecraft compared to that of the planets [15]. This approximation can be made because the forces other celestial bodies apply to the spacecraft are negligible compared to that of the sun. This same approximation can be made in a spacecraft-planet or spacecraft-moon

system if the spacecraft is within the sphere of influence (SOI) of the body, where the gravitational pull of Jupiter becomes greater than the gravitational pull of the sun. Equation (2.2) calculates the SOI for a body with respect to another body.

$$r_{SOI} = r\left(\frac{m_2}{m_1}\right)^{0.4} \tag{2.2}$$

Where r is the distance between the two masses, and m_2 is the smaller of the two masses.

When the two-body approximation is made, the simple two-body dynamics equations can be used. The primary equation used in two-body mechanics is derived using Newton's second law and Eq (2.1), and is given in Eq. (1.3)

$$\ddot{\mathbf{r}} = \frac{-G(m_1 + m_2)}{r^3}\mathbf{r} \tag{2.3}$$

Equation (2.3) is the differential equation of the relative motion of the spacecraft and the body it is orbiting, however since the gravitational pull of the spacecraft on the body is negligible, it is assumed that only the spacecraft is actually in motion. The variable **r** is the radius vector, and the variable r is the radius magnitude. The gravitational parameter μ is found by multiplying the combined mass of the body and the spacecraft with the gravitational constant, G. Equation (2.3) is a simple differential equation that relates the motion of the smaller body with respect to the larger [14]. The energy equation can be obtained via a few mathematical steps and is given in Eq. (2.4)

$$\frac{V^2}{2} - \frac{\mu}{r} = E \tag{2.4}$$

Where V is the velocity of the spacecraft and E is the total mechanical energy of the orbit.

In order to be able to calculate the six orbital elements, application of the equations of conic sections is necessary. The polar equation of a conic section is given in Eq. (2.5).

$$r = \frac{p}{1 + \varepsilon \cos \nu} \tag{2.5}$$

Where p is semilatus rectum of the orbit, ε is the eccentricity, and ν is the true anomaly. When the semilatus rectum is related to the size and shape of the orbit, equations calculating the minimum (periapsis) and maximum (apoapsis) radius of the orbit are acquired. Equations (2.6-2.8) relate these values.

$$p = a(1 - \varepsilon^2) \tag{2.6}$$

$$r_p = \frac{p}{1 + \varepsilon} \tag{2.7}$$

$$r_a = \frac{p}{1 - \varepsilon} \tag{2.8}$$

Where r_p is the radius of periapsis and r_a is the radius of apogee.

The angular momentum of a spacecraft can be found at the apsides by simply finding the product of the distance and velocity as shown in Eq. (2.9)

$$H = r_p V_p = r_a V_a \tag{2.9}$$

Where H is the angular momentum. Relating all of the above equations together, a simple relationship between the energy of the system and semimajor axis can now be made, and is given in Eq. (2.10) [14].

$$E = \frac{-\mu}{2a} \tag{2.10}$$

The direction of the velocity vector with respect to the local horizon is known as the flight path angle, Φ. The flight path angle is needed when using tangential thrust

because the thrusters must be pointed along the velocity vector, not the local horizon. Equation (2.11) calculates the flight path angle [15].

$$\Phi = \cos^{-1}\left(\frac{H}{rV}\right) \tag{2.11}$$

Now that all of the sizing and shaping elements can be found, the elements that orientate the orbit in three-dimensional space need to be examined. The inclination is the angle between the orbit plane with respect to the equatorial plane, which is the same angle as between the polar axis and the angular momentum vector. The inclination angle is measured in a counterclockwise direction and only ranges from 0-180 deg. Equation (2.12) gives the equation for the inclination

$$i = \cos^{-1}\left(\frac{\mathbf{K}\cdot\mathbf{H}}{H}\right) \tag{2.12}$$

when the orbital plane and the equatorial plane cross, the line of nodes is formed. The ascending node is where the spacecraft crosses the equatorial plane from below. The next variable needed to orientate the orbit is the right ascension of the ascending node. The right ascension of the ascending node is the angle counterclockwise between the vernal equinox and the ascending node and is given in Eq. (2.13).

$$\Omega = \cos^{-1}\left(\frac{\mathbf{I}\cdot\mathbf{n}}{n}\right) \tag{2.13}$$

The final orbital element needed is the argument of periapsis. The argument of periapsis arranges the two dimensional orbit found with the semimajor axis and eccentricity, on the orbital plane found using the inclination and the right ascension of the ascending node. The argument of periapsis is the angle between the ascending node and periapsis [15]. The formula is given in Eq. (2.14).

$$\omega = \cos^{-1} \frac{\mathbf{n} \cdot \vec{\varepsilon}}{n\varepsilon} \tag{2.14}$$

Using Eqs (2.4-2.14), the six classical orbital elements can now be found. With these elements and the simple energy equations, all orbits can be found for the simplified two-body case.

Three-Body Problem

Although it is a reasonable approximation to assume two-body mechanics when a spacecraft is within only one body's sphere of influence, not all locations in the solar system are so simple. For instance, take a spacecraft traveling from Earth to the moon, when the spacecraft first leaves Earth two-body mechanics with the Earth and the spacecraft are reasonable due to the drastic greater amount of Earth's gravitational pull, however as the spacecraft approaches the moon, the gravity of the moon must be considered as well as the gravity of the Earth because of the moon's increasing gravitational pull as the spacecraft gets closer to the moon. When more than one body is influencing the spacecraft, N-body dynamics must be used. This will be the case when the spacecraft is rendezvousing with each of the Galilean moons it needs to visit. For simplicity it will be assumed that only three bodies will be involved in stating the equations: the spacecraft, the planet, and the moon. This problem is the description of motion of an infinitesimal mass being influenced by two massive bodies which revolve around their center of mass [16]. First, the angular velocity of the bodies must be found using Eq. (2.15).

$$\omega^2 = \frac{G(m_1 + m_2)}{r_{12}^{\ 3}} \tag{2.15}$$

Where r_{12} is the constant distance between the two masses. Now a coordinate frame that has the origin at the center of mass, the x axis is between the two bodies centers of masses, and the coordinate frame rotates with velocity ω is created [16]. Equation (2.16) gives the position of the spacecraft in the system.

$$\vec{\rho}_1 = \vec{r} - \vec{r}_1 \qquad\qquad \vec{\rho}_2 = \vec{r} - \vec{r}_2 \tag{2.16}$$

Where $\vec{r}$ is the distance vector from the spacecraft to the center of mass, and $\vec{r}_1$ and $\vec{r}_2$ are the radii to the respective bodies. Next, an equation of motion can be established in within the given coordinate system and is given in Eq. (2.17).

$$\frac{d^2\vec{r}}{dt^2} + 2\vec{\omega} \times \frac{d\vec{r}}{dt} + \vec{\omega} \times (\vec{\omega} \times r) + \frac{Gm_1}{\vec{\rho}_1^{\ 3}}\vec{\rho}_1 + \frac{Gm_2}{\vec{\rho}_2^{\ 3}}\vec{\rho}_2 = 0 \tag{2.17}$$

Now that the equation of motion has been found, Jacobi's integral can be discussed. Jacobi determined an energy-like integral for the equation of motion by defining the scalar function given in Eq. (2.18) [17].

$$J = \frac{\omega^2}{2}\left(\xi^2 + \zeta^2\right) + \frac{Gm_1}{\rho_1} + \frac{Gm_2}{\rho_2} \tag{2.18}$$

Where ξ and ζ are the positions of the spacecraft in the rotating plane. This function when written in terms of the gradient is perfectly differential, and integrating the equation gives a modified energy equation for three-body given in Eq. (2.19) known as Jacobi's integral [17].

$$V_{rel}^{\ 2} = \omega^2\left(\xi^2 + \zeta^2\right) + \frac{2Gm_1}{\rho_1} + \frac{2Gm_2}{\rho_2} - C \tag{2.19}$$

Where V_{rel} is the magnitude of the observed velocity and C is the constant of integration. The value of the constant of integration defines the type of orbit that the spacecraft has revolving around the center of mass.

There are several different ways that the spacecraft can orbit the two bodies. Figure 2.1 shows the different types of orbits that a spacecraft can have. In Jacobi's function there are points at which $\partial J/\partial \xi = \partial J/\partial \eta = 0$. If the spacecraft is placed at rest in the rotating plane in one of these points, its acceleration will be zero; therefore it would remain at rest forever unless it is acted upon by an external force. There are five points at which the conditions for zero acceleration are satisfied. These five points are called the libration points, L1-L5. Figure 2.1 shows the five libration points [18].

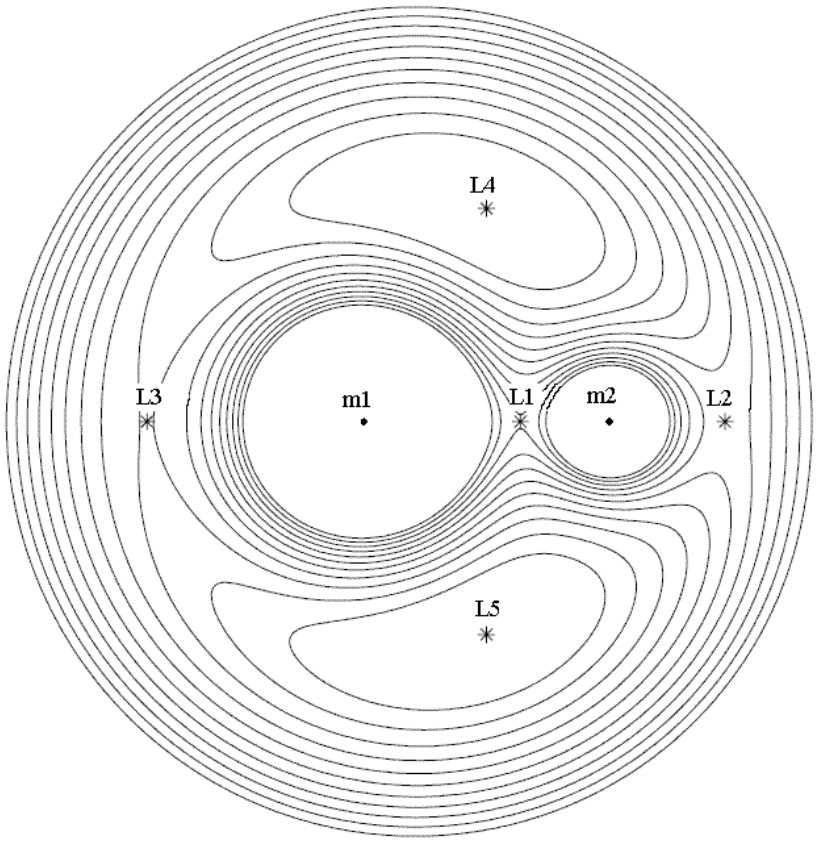

Figure 2.1. *Surfaces of zero velocity and libration points for three-body problem.*

The libration point between the planet and the moon is a very important libration point. When a spacecraft starts in a very low-energy initial orbit about the moon and thrusts to increase energy, once the libration point between the planet and the moon has been crossed, the orbit shape is drastically changed due to the gravitational pull of the planet. This libration point, L1, is calculated using μ_{L1} which is a combination of the gravitational parameters of the planet and the moon. The L1 point and μ_{L1} are calculated in Eqs. (2.20)-(2.21) [16].

$$L1 = \left(\frac{\mu_{L1}}{3}\right)^{\frac{1}{3}} + \frac{1}{3\left(\left(\frac{\mu_{L1}}{3}\right)^{\frac{1}{3}}\right)^{2}} - \frac{1}{9\left(\left(\frac{\mu_{L1}}{3}\right)^{\frac{1}{3}}\right)^{3}} \tag{2.20}$$

$$\mu_{L1} = \frac{\mu_m}{\left(\mu_m + \mu_{pl}\right)} \tag{2.21}$$

With the three-body equation of motion, and Jacobi's integral, the trajectory of a spacecraft can be found in a three-body system.

Relative Acceleration Method

An equation for the acceleration of the spacecraft with respect to the moon can be developed using first principles. For the derivation in this section the moon will be body one, Jupiter is body two, and the spacecraft is body three. The origin of the coordinate system is the barycenter of the Jupiter-moon system. The barycenter is the center of mass between the two bodies. Vectors between bodies are defined as

$$\vec{\rho}_{12} = \vec{r}_2 - \vec{r}_1 \tag{2.22}$$

$$\vec{\rho}_{13} = \vec{r}_3 - \vec{r}_1 \tag{2.23}$$

$$\vec{\rho}_{23} = \vec{r}_3 - \vec{r}_2 \tag{2.24}$$

Where $\vec{r}_1$, $\vec{r}_2$, and $\vec{r}_3$ are vectors from the barycenter to the moon, Jupiter, and the spacecraft respectively. Using Eq. (2.1) the equation of motion for each of the bodies can be found, and are given in Eqs. (2.25)-(2.27).

$$m_1\ddot{\vec{r}}_1 = \frac{Gm_1m_2}{\rho_{12}^3}\vec{\rho}_{12} + \frac{Gm_1m_3}{\rho_{13}^3}\vec{\rho}_{13} \tag{2.25}$$

$$m_2\ddot{\vec{r}}_2 = -\frac{Gm_2m_1}{\rho_{12}^3}\vec{\rho}_{12} + \frac{Gm_2m_3}{\rho_{23}^3}\vec{\rho}_{23} \tag{2.26}$$

$$m_3\ddot{\vec{r}}_3 = -\frac{Gm_3m_1}{\rho_{13}^3}\vec{\rho}_{13} - \frac{Gm_3m_2}{\rho_{23}^3}\vec{\rho}_{23} \tag{2.27}$$

Now that the accelerations with respect to the barycenter can be found, the acceleration of the spacecraft with respect to the moon can be found by combining the second derivative of Eq (2.23) with Eqs. (2.25-2.27), and is given in Eq. (2.28).

$$\ddot{\vec{\rho}}_{13} = -\frac{Gm_1}{\rho_{13}^3}\vec{\rho}_{13} - \frac{Gm_2}{\rho_{23}^3}\vec{\rho}_{23} - \frac{Gm_2}{\rho_{12}^3}\vec{\rho}_{12} \tag{2.28}$$

Equation (2.28) simply includes the gravitational forces that each of the bodies apply to the spacecraft. In order for this equation to be used in propagating an orbit, the acceleration vector from thrust must also be included in the equation.

Thruster Performance

When evaluating the performance of a thruster there are four main variables to consider: thrust (T), specific impulse (I_{sp}), mass flow rate ($\dot{m}$), and effective exhaust velocity (c). For electric propulsion, thrust is the force produced by the input power of the rocket (P). The specific impulse of a rocket is the change in momentum per unit of propellant. Specific impulse is a value that determines the efficiency of the rocket. Mass flow-rate is how quickly the fuel is used. Effective exhaust velocity is thrust per mass flow-rate. These variables are directly related to each other. Their relationships are given in Eqs. (2.29-2.31) [14].

$$I_{sp} = \frac{T}{\dot{m} g_o} \tag{2.29}$$

$$c = I_{sp} g_o \tag{2.30}$$

$$T = \dot{m} c = \dot{m} g_0 I_{sp} \tag{2.31}$$

Where g_o is the gravitational constant on Earth. With these variables, the rocket equation can now be used. The rocket equation calculates the mass ratio before and after firing the engines. The rocket equation is

$$\frac{m_i}{m_f} = \exp\left(\frac{\Delta V}{c}\right) \tag{2.32}$$

Where ΔV is the propulsive effort required to get from one point to another.

Now that the mass ratio can be found, a comparison between chemical and electric propulsion engines will be examined. Chemical engines are naturally high-thrust engines, and they also have high mass flow-rates. This leads to chemical engines having

a relatively low value for specific impulse. The standard specific impulse of a chemical engine is around 175-300 s [19]. Electric propulsion on the other hand are naturally low-thrust engines, and they have very small mass flow-rates. The specific impulse for electric propulsion engines can be around ten times greater than that of chemical engines. The standard specific impulse for an electric propulsion engine can range from 3000-7000 s depending on the type of thruster used. Deep Space 1 used a thruster that had a specific impulse of 3000 s [20]. The JIMO mission has two different thrusters; the spacecraft has both engines around 3000 s and some with specific impulses of 7000 s, which allows for greater thrust at some times and greater efficiency at others [8]. The fact that electric propulsion engines have a greater specific impulse makes the mass ratio for the low-thrust engines much better than that for the high thrust engines; however the gaining of final mass comes at a cost of increased trip time due to the lower thrust.

Final Mass Calculations

The final mass of the spacecraft is simply the initial mass minus the mass of propellant consumed. However the amount of mass that is usable for science purposes is the number that scientists are interested in. The final mass is divided five ways: science mass m_{sc}, tank mass m_t, structure mass m_{st}, power system mass m_{pp}, and radiation shield mass m_{rs} [21]. The structural mass can be computed as purely a percentage of the initial mass, and therefore the structural mass is considered independent of the other sections of the final mass [22]. The tank mass is calculated simply as a percentage of the amount of propellant consumed by the spacecraft, and the power system mass is proportional to the

power level of the thrusters used [23]. The radiation shielding can roughly be calculated as a percentage of the initial mass as well [24].

$$m_{st} = K_{st} m_0 \tag{2.33}$$

$$m_t = K_t m_{prop} \tag{2.34}$$

$$m_{pp} = K_{pp} P \tag{2.35}$$

$$m_{rs} = K_{rs} m_0 \tag{2.36}$$

The vehicle parameters K_{st}, K_t, and K_{pp} are considered constant for nuclear electric propulsion spacecraft [25,26]. The current technology level for space nuclear power and ion thrusters are scaled, and the vehicle parameters are derived by using References 22,25,26. A scaled-up reactor system for the multimegawatt power range is presented in Ref. 25. Constant values for the parameters are given below.

$$K_{st} = 0.08$$

$$K_t = 0.05$$

$$K_{pp} = 7.3 \text{ kg/kW}$$

$$K_{rs} = 0.10$$

Using these sizing parameters the science mass of the spacecraft can now be calculated in Eq. (2.37).

$$m_{sc} = (1 - K_{st} - K_{rs}) m_0 - (1 + K_t) m_{prop} - K_{pp} P \tag{2.37}$$

Approximate Low-Thrust Transfers

When a spacecraft is using electric propulsion engines to either escape a body or capture into one, the spacecraft has to do many quasi-circular spirals around the body. In the celestial mechanics section, equations were given that allow calculation of these spirals; however due to the number of spirals involved, the integration time needed is very large. In order to lessen the computational load, method of numerical estimation is needed. Gao and Kluever developed a method of orbital averaging that allows for an analytic calculation of the orbital elements, which saves computational time [27]. Their method of orbital averaging is only valid for elliptic orbits, and the method is a two-body dynamics method. The way in which the elements are approximated is that an analytic rate of each orbital element is averaged over an entire revolution. The Gauss planetary equations give the rate of change of each of the orbital elements with respect to time. They are given in Eqs. (2.38)-(2.43).

$$\frac{da}{dt} = \frac{2a^2 e \sin\theta}{h} f_r + \frac{2a^2 p}{hr} f_\theta \tag{2.38}$$

$$\frac{de}{dt} = \frac{1}{h} p \sin\theta \; f_r + \frac{1}{h}[(p+r)\cos\theta + re] f_\theta \tag{2.39}$$

$$\frac{di}{dt} = \frac{r\cos(\omega+\theta)}{h} f_n \tag{2.40}$$

$$\frac{d\Omega}{dt} = \frac{r\sin(\omega+\theta)}{h\sin i} f_n \tag{2.41}$$

$$\frac{d\omega}{dt} = -\frac{p\cos\theta}{he} f_r + \frac{(p+r)\sin\theta}{he} f_\theta - \frac{r\sin(\omega+\theta)\cos i}{h\sin i} f_n \tag{2.42}$$

$$\frac{dM}{dt} = n + \frac{1}{ahe}\left[(p\cos\theta - 2re) f_r - (p + r)\sin\theta\ f_\theta\right] \tag{2.43}$$

where
$$h = \sqrt{\mu p} \tag{2.44}$$

$$n = \sqrt{\frac{\mu}{a^3}} \tag{2.45}$$

However, the eccentric anomaly will be used as the sixth orbital element instead of the mean anomaly, and is given in Eq (2.46)[27].

$$\frac{dE}{dt} = \frac{na}{r} + \frac{1}{nae}[f_r(\cos\theta - e) - f_\theta(1 + \frac{r}{a})\sin\theta] \tag{2.46}$$

The derivative of eccentric anomaly with respect to time can be approximated when using low-thrust acceleration by removing the term related to thrust, and the simplification is given in Eq. (2.47).

$$\frac{dE}{dt} \approx \frac{na}{r} \tag{2.47}$$

Using Eq. (2.47) and the Gauss planetary equations, the derivatives of all the classical orbital elements with the exception of true anomaly can be calculated with respect to the eccentric anomaly [27].

$$\frac{da}{dE} = \frac{2a^3}{\mu}\left(f_r e\sin E + f_\theta\sqrt{1 - e^2}\ \right) \tag{2.48}$$

$$\frac{de}{dE} = \frac{a^2}{\mu}\left(f_r(1-e^2)\sin E + f_\theta(2\cos E - e - e\cos^2 E)\sqrt{1-e^2}\ \right) \tag{2.49}$$

$$\frac{di}{dE} = \frac{a^2}{\mu} f_n\left(\frac{\cos\omega\cos E - e\cos\omega}{\sqrt{1-e^2}} - \sin\omega\sin E\ \right)(1-e\cos E) \tag{2.50}$$

$$\frac{d\Omega}{dE} = \frac{a^2}{\mu} f_n\left(\frac{\sin\omega\cos E - e\sin\omega}{\sqrt{1-e^2}} + \cos\omega\sin E\ \right)\frac{(1-e\cos E)}{\sin i} \tag{2.51}$$

$$\frac{d\omega}{dE} = -\cos i\frac{d\Omega}{dE} - \frac{a^2}{e\mu}\left(f_r(\cos E - e)\sqrt{1-e^2} - f_\theta(2-e^2-e\cos E)\sin E\right) \tag{2.52}$$

Now that the orbital elements are expressed in terms of the change with respect to eccentric anomaly, the final step is to integrate Eqs. (2.48)-(2.52) with respect to the eccentric anomaly over a single revolution. Equations (2.53)-(2.57) are the equations for the rate of change of each orbital element with respect to eccentric anomaly.

$$\int_{E_0}^{E_f}\frac{da}{dE}dE = \frac{2a^3}{\mu} f_{in}\int_{E_0}^{E_f}\sqrt{1-e^2\cos^2 E}\,dE \tag{2.53}$$

$$\int_{E_0}^{E_f}\frac{de}{dE}dE = \frac{2a^3}{e\mu}(1-e^2) f_{in}\left\{\begin{array}{l}\displaystyle\int_{E_0}^{E_f}\sqrt{1-e^2\cos^2 E}\,dE - \int_{E_0}^{E_f}\frac{1}{\sqrt{1-e^2\cos^2 E}}dE \\ \displaystyle + \left[\ln(\sin E + \frac{1}{e}\sqrt{1-e^2\cos^2 E})\right]_{E_0}^{E_f}\end{array}\right\} \tag{2.54}$$

$$\int_{E_0}^{E_f}\frac{di}{dE}dE = \frac{a^2}{\mu} f_n\left[\begin{array}{r}\displaystyle\frac{(1+e^2)\cos\omega\sin E - 1.5eE\cos\omega - 0.25e\cos\omega\sin 2E}{\sqrt{1-e^2}} \\ + \sin\omega\cos E - 0.25e\sin\omega\cos 2E\end{array}\right]_{E_0}^{E_f} \tag{2.55}$$

$$\int_{E_0}^{E_f}\frac{d\Omega}{dE}dE = \frac{a^2}{\mu\sin i} f_n\left[\begin{array}{r}\displaystyle\frac{(1+e^2)\sin\omega\sin E - 1.5eE\sin\omega - 0.25e\sin\omega\sin 2E}{\sqrt{1-e^2}} \\ - \cos\omega\cos E + 0.25e\cos\omega\cos 2E\end{array}\right]_{E_0}^{E_f} \tag{2.56}$$

$$\int_{E_0}^{E_f} \frac{d\omega}{dE} dE = -\frac{2a^2}{e^2 \mu} \sqrt{1-e^2}\, f_{in} \left[\sqrt{1-e^2 \cos^2 E} + \arcsin(e \cos E) \right]_{E_0}^{E_f} - \cos i \int_{E_0}^{E_f} \frac{d\Omega}{dE} dE \quad (2.57)$$

Where f_{in} is the in-plane thrust and f_n is the thrust normal to the plane. The integrals are being calculated from E_0 to E_f which are the exit and entrance of the shadow angle. The shadow is when the spacecraft is behind the planet relative to the sun. When solar electric propulsion is being used, the power that the engine has when in the shadow region is zero, however in nuclear electric propulsion the shadow doesn't need to be considered, and the integrals are simply integrated from zero to 2π. Analytic expressions for the terms $\int_{E_0}^{E_f} \sqrt{1-e^2 \cos^2 E}\, dE$ and $\int_{E_0}^{E_f} \frac{1}{\sqrt{1-e^2 \cos^2 E}} dE$ are unable to be found, however the two terms can also be approximated by Eqs. (2.58-2.59).

$$\begin{aligned} \int_{E_0}^{E_f} \sqrt{1-e^2 \cos^2 E}\, dE &\approx \int_{E_0}^{E_f} \left(\sqrt{1-e^2} + (1-\sqrt{1-e^2}) \sin^2 E \right) dE \\ &= \left[\sqrt{1-e^2}\, E + (1-\sqrt{1-e^2})(0.5E - 0.25 \sin 2E) \right]_{E_0}^{E_f} \end{aligned} \quad (2.58)$$

$$\begin{aligned} &\int_{E_0}^{E_f} \sqrt{1-e^2 \cos^2 E}\, dE - \int_{E_0}^{E_f} \frac{1}{\sqrt{1-e^2 \cos^2 E}} dE = \int_{E_0}^{E_f} \frac{-e^2 \cos^2 E}{\sqrt{1-e^2 \cos^2 E}} dE \\ &\approx \int_{E_0}^{E_f} \frac{-e^2 \cos^2 E}{\sqrt{1-e^2 c}} dE = \frac{-e^2}{\sqrt{1-e^2 c}} \left[0.5E + 0.25 \sin 2E \right]_{E_0}^{E_f} \end{aligned} \quad (2.59)$$

The results of the algorithm match that of full integration well for multiple different initial orbits. All of the orbital elements, as well as flight time, can be approximated via the orbital averaging method except one, true anomaly. The true anomaly, angular position of the spacecraft, is lost in Gao and Kluever's method. This occurs due to the averaging the orbital elements instead of actually calculating the trajectory. Once the differential change in the elements is calculated, the differential amount is added on to

the current orbit, and the orbit is updated having completed one revolution around Jupiter. This process is repeated until a final value specified by the user is achieved. Orbital averaging works well for escape and capture trajectories involving multiple spirals. However, orbital averaging begins to break down on the final revolutions of an escape trajectory, or the first revolutions on a capture trajectory, due to rapid time-rate gain of variables such as eccentricity, as well as the increased period, which makes the amount of time being estimated at once increase drastically near escape conditions. Therefore orbital averaging is used until the final value requirement is nearly achieved, and then the algorithm steps back a desired number of revolutions, prescribed by the user, and uses standard integration of the complete equations of motion for the last few revolutions.

Another analytic method was derived by Edelbaum. Edelbaum derived a formula to calculate the change in ΔV for a spacecraft going from one circular orbit to another [28]. The equation simply takes into account the initial and final velocities of the spacecraft, as well as the change in inclination, and is given in Eq. (2.60). Edelbaum's equation assumes that nuclear electric propulsion is being used, and therefore there is no shadow consideration necessary.

$$\Delta V = \sqrt{V_i^2 + V_f^2 - 2V_i V_f \cos\left(\frac{\Delta i \pi}{2}\right)} \tag{2.60}$$

This equation only holds true for inclination changes of around 30 degrees or less. Edelbaum's equation simply reduces to the difference between the initial and final orbit velocities for trajectories with no inclination change [28].

SNAP

NASA Glenn Research Center (GRC) has an N-body integration program that can integrate trajectories about any body in the solar system. The program is named Spacecraft N-Body Analysis Program (SNAP). Trajectories in SNAP are propagated using a Runge-Kutta-Fehlberg single-step method with variable step-size control using an 8^{th}-order method and comparing the solution to a 7^{th}-order method to obtain an estimate of the truncation error [29]. SNAP uses ephemeris data provided by NASA to determine the location of all the bodies in the solar system at all times [30]. SNAP has the ability to turn the gravity of any body in the solar system "on" or "off"; therefore the differences between a two-body trajectory for a spacecraft in a system, and a three-body trajectory can be compared [29]. For example, a spacecraft is initially in a low orbit about Europa and it needs to use low-thrust spirals to escape. In order to test the feasibility of using two-body dynamics to escape, two cases are run: a two-body case with the spacecraft and Europa, and a three-body case with Jupiter included. These trajectories can now be compared to find if two-body dynamics are suitable. SNAP needs only the initial conditions of the spacecraft, and then it simply integrates the N-body equations out to a given final stopping condition. Stopping conditions can be almost anything desired from a specified energy, final radius, final eccentricity, to something as simple as final time [29]. SNAP does not have the ability to optimize a trajectory though; SNAP is purely an integrator and trajectory propagator. SNAP has the ability to output all of the states of the orbit at all times in the trajectory; therefore the orbits can be compared at any time in

the trajectory not just at the beginning and the end. SNAP can be used as a useful tool to find trajectories for known initial conditions.

CHAPTER 3 NUMERICAL RESULTS

Rendezvousing with Initial Moon

The spacecraft starts with an initial condition of just entering Jupiter's sphere of influence and being captured into a parabolic, planar orbit about Jupiter's barycenter. From this point, the spacecraft must now rendezvous with the first Galilean moon that it is required to, Callisto, in order to collect data on the moon. In order for the spacecraft to rendezvous with the moon using electric propulsion, the spacecraft must follow many revolutions about Jupiter. These revolutions take a very large computational load, and in order to lessen the load, an analytic approach must be taken. The orbital averaging method discussed in Section 2.3 will be used. Jupiter's sphere of influence is $48.2(10^6)$ km, which was calculated with Eq. (2.2). Therefore, the spacecraft arrives at the sphere of influence with an eccentricity of unity and needs to arrive at Callisto's orbit which has a radius of $1.883(10^6)$ km and is circular (eccentricity equal to 0). The final mass and time are calculated with orbital averaging for several different initial masses and thrusts, and the results are displayed in Table 3.1.

Table 3.1. *Final mass and time for spacecraft to travel from parabolic trajectory at SOI to circular trajectory at Callisto with different masses and thrusts.*

		Orbital Averaging	
Initial Mass0 (kg)	**Power (kW)**	**Final Mass (kg)**	**Transfer Time (days)**
1000	10	796.4	160.5
1000	15	803	98.55
1000	20	809.2	62.4
2000	10	1562.8	339.45
2000	15	1577.3	219
2000	20	1592.8	160.6
3000	10	2296.5	546.8
3000	15	2328.1	349.5
3000	20	2345.6	252
5000	10	3812.3	927
5000	15	3850.7	602.6
5000	20	3851.4	445.6
10000	50	9046	740.95
10000	100	9097.1	350.4
20000	60	18019	1284.8
20000	100	18092	740.95
30000	50	27006	2332.35
30000	100	27093	1131.5

The cases when the spacecraft starts with 5000 kg or less initial mass have specific impulses of 2700 s and efficiencies (η) of 50 %. The thrust of the engine is found with Eq (3.1).

$$T = \frac{2\eta P}{g_0 I_{sp}} \tag{3.1}$$

The spacecraft that start with 10,000 kg or more of initial mass have a higher specific impulse of 7000 s and also have a greater efficiency of 70 %. These spacecraft have improved specifications for future missions assuming the technologies will continue to improve. The trajectories of each of the different situations given in Table 3.1 are similar. All of the trajectories begin as a parabola and quickly become circular and remain circular all the way until Callisto's orbit is reached. Figure 3.1 shows the first few

revolutions of the trajectory for the nominal case of 5000 kg initial mass and 15 kW power.

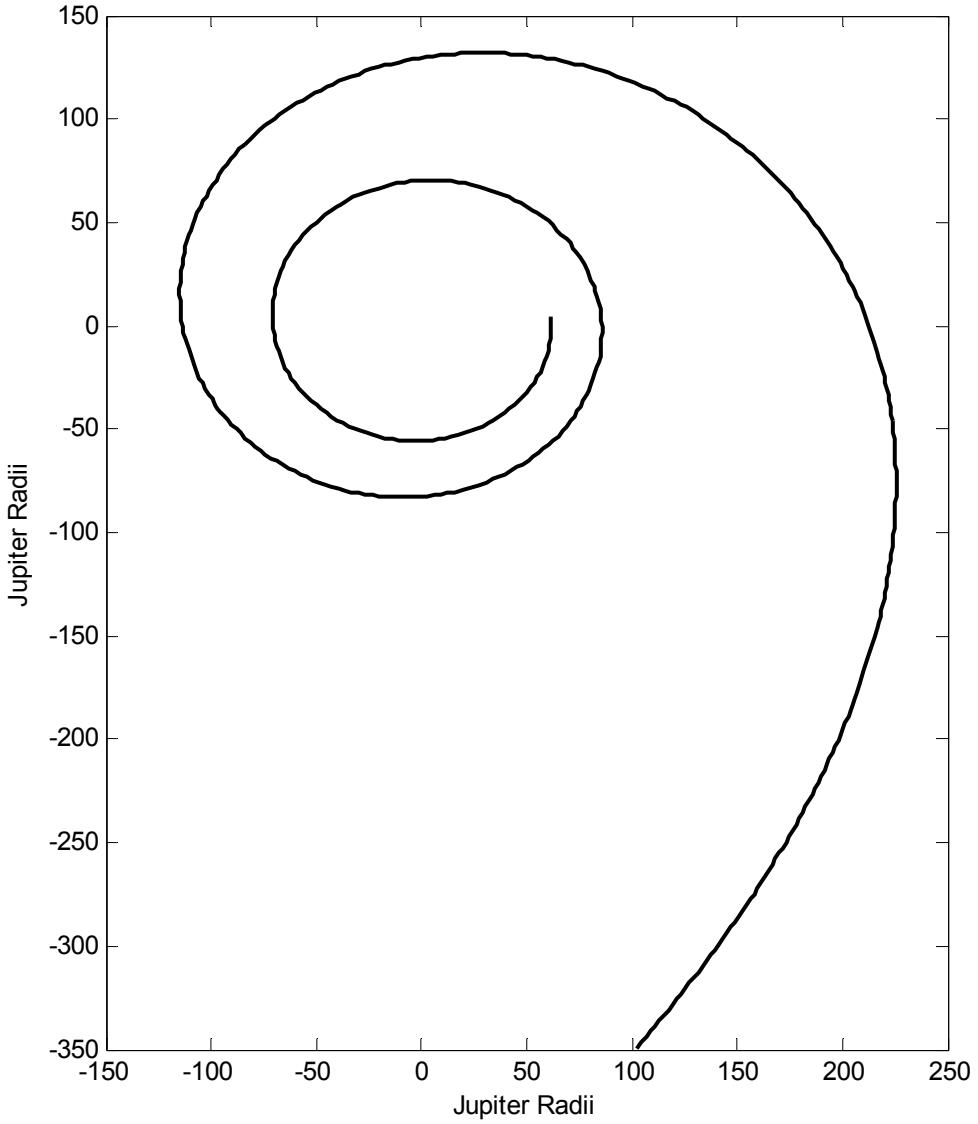

Fig. 3.1. *First few revolutions of a spacecraft entering Jupiter's SOI as parabola and tangentially thrusting down to Callisto's orbit with initial mass 5000 kg and power of 15 kW.*

In order to understand how the orbital elements are changing as the trajectory evolves from a parabola to a circle, graphs of the eccentricity and energy of the orbit with respect to the trip time are given in Figs 3.2-3.3 respectively. Arrival time at Callisto's orbit is time zero and the same nominal condition as above is used.

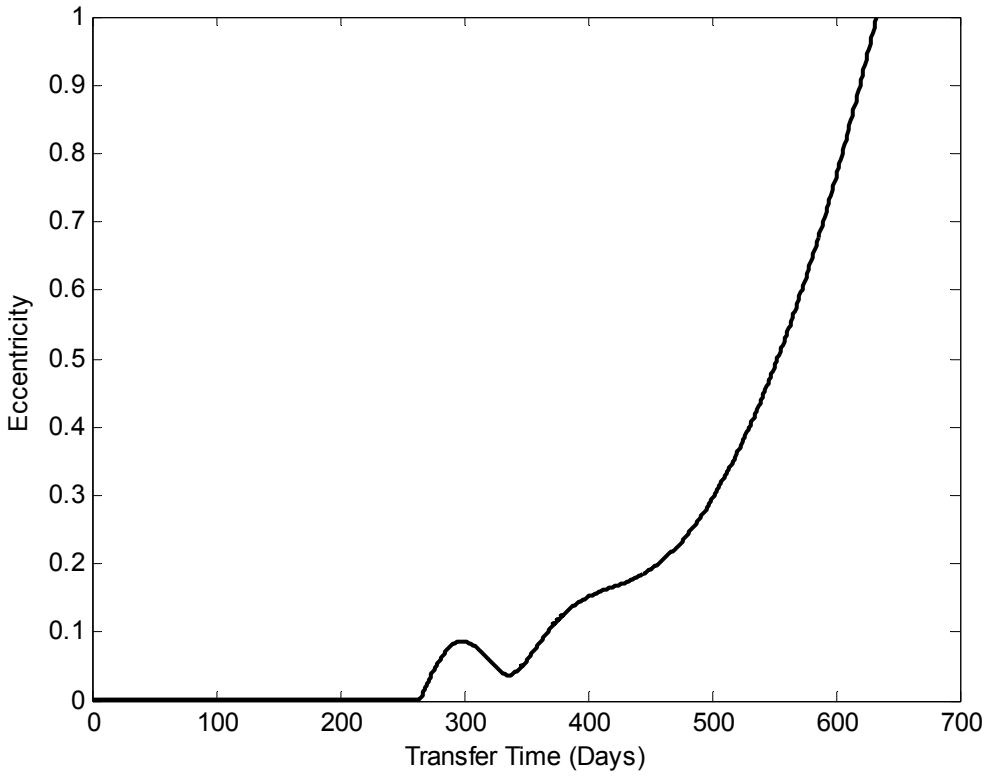

Fig. 3.2. *Eccentricity vs. transfer time for a spacecraft entering Jupiter's SOI as parabola and tangentially thrusting down to Callisto's orbit with initial mass 5000 kg and power of 15 kW.*

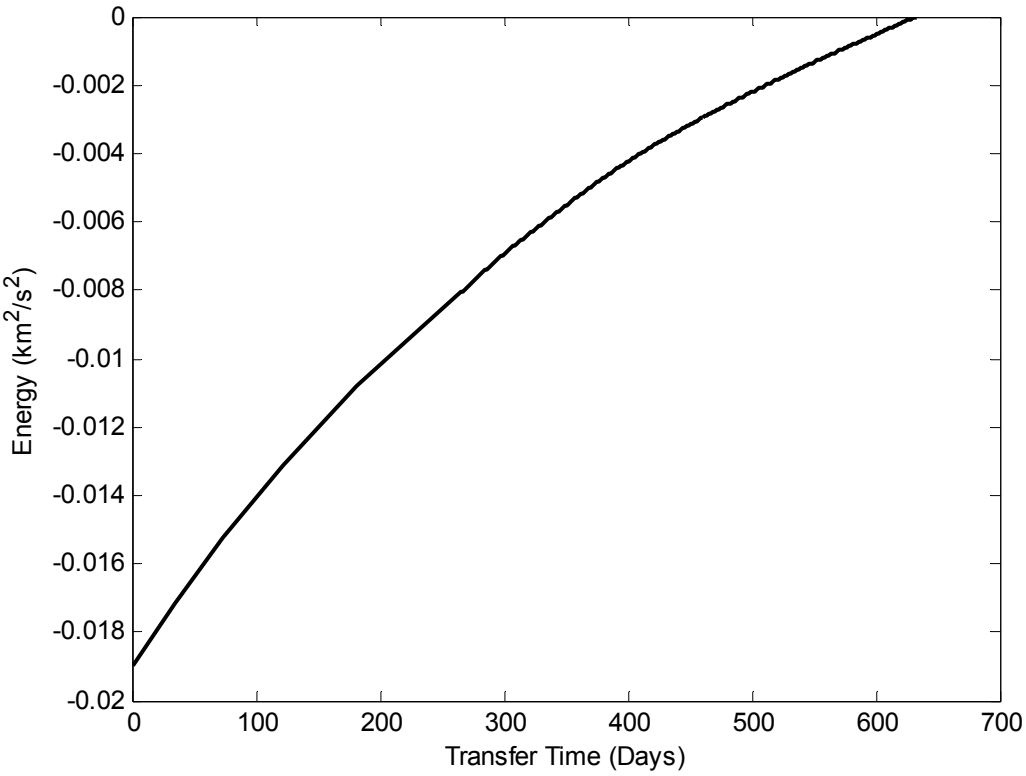

Fig. 3.3. *Energy vs. transfer time for a spacecraft entering Jupiter's SOI as parabola and tangentially thrusting down to Callisto's orbit with initial mass 5000 kg and power of 15 kW .*

The eccentricity of the orbit appears to be unchanging for about half of the trajectory, this is due to the orbit having circularized and orbital averaging being used. Figure 3.1 shows that the orbit does circularize in about two revolutions. When the eccentricity begins to change the spacecrafts orbit is beginning to have a great time-rate of change. The rate of change requires for integration to be used, therefore the eccentricity of the orbit is followed explicitly. The energy of the orbit is constantly decreasing due to the tangential steering with the thrust pointing against the velocity.

The energy of the orbit starts at zero which is a non-captured trajectory. The transfer time of the orbit can be decreased by increasing power.

Capture into / Escape from Moons

Tangential Steering

Once the spacecraft has reached Callisto's orbit, the next step in the moon tour is to capture into a low orbit about Callisto. The first step is to align the spacecraft's true anomaly with Callisto. This, however, takes virtually no time or mass when considering the entire trip due to the short period that each of the moons has compared to the total trip time. Callisto has the longest period of the moons by over double and it revolves around Jupiter every 16.7 days. If the spacecraft is given slight corrective maneuvers in the final approach to the moon aligning the spacecraft and the moon would add no more than a couple of days total trip time. Comparing a few days to just the approach to Callisto, which takes over a year for feasible solutions, much less the entire mission, shows that this part of the trajectory can be ignored when the time and mass for the mission are purely being estimated.

Now that the spacecraft has rendezvoused with Callisto, the next step is to capture the spacecraft into an orbit about Callisto from an orbit around Jupiter. The first approach taken to do this is using orbital averaging to capture into the moon. The two-body trajectory that captures into the moon has to start outside the moon's sphere of influence with respect to Jupiter in order for moon to be able to capture the spacecraft. This poses a problem because the spacecraft is across the L1 libration point at this time;

therefore the spacecraft is not purely in an orbit about the moon. In order to check the accuracy of using orbital averaging to calculate the capture trajectory of a spacecraft into the moons, the two-body results from orbital averaging are compared to the three- body results calculated by SNAP. Figure 3.4 shows the radius of the spacecraft with respect to the mass of the spacecraft for all of the two-body and the three-body situations. Figure 3.4 is an escape trajectory, not a capture trajectory, however these two phases are treated very similarly, and the problem with Jupiter's gravitational pull occurs equally in both. The escape trajectory data from each of the Galilean moons is shown in Fig. 3.4. In this nominal case, the initial mass is 2000 kg and the power level is 60 kW and the specific impulse is 2700 s.

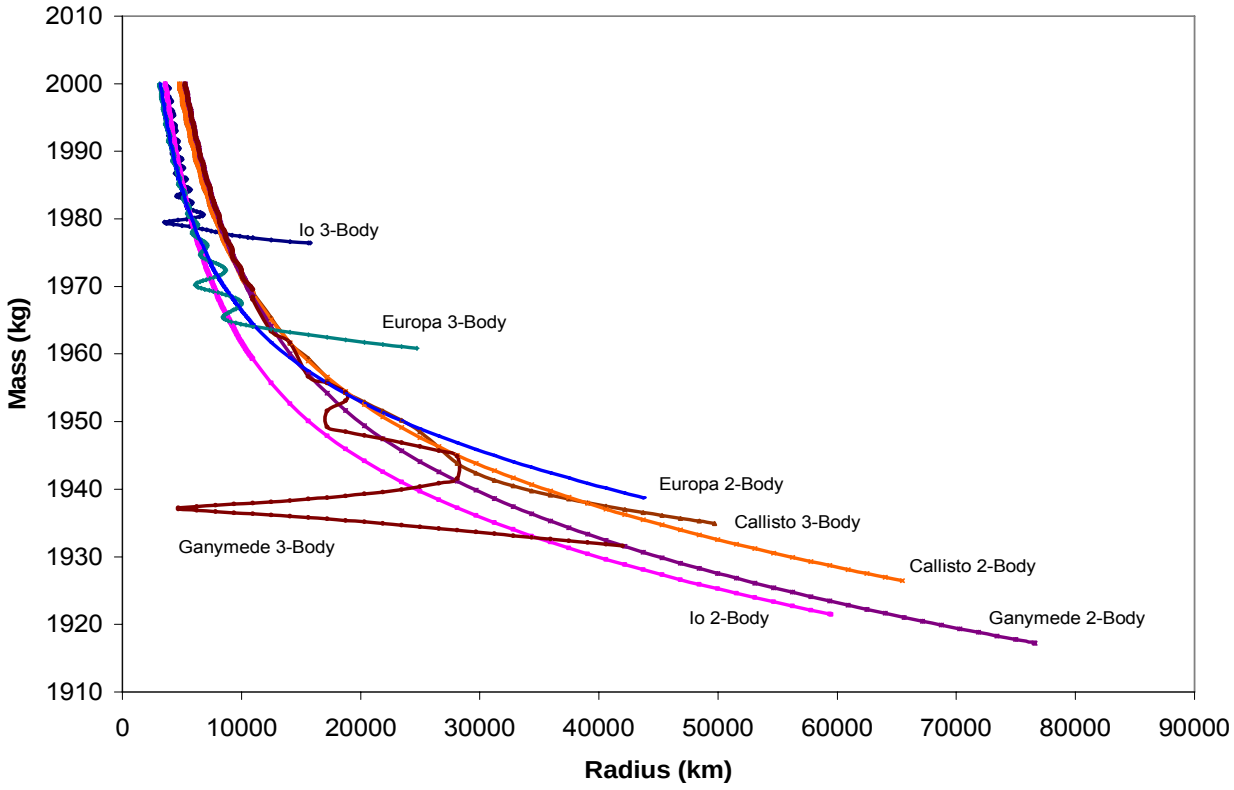

Fig. 3.4. *Two and three-body mass vs. radius of the spacecraft data for a spacecraft with 2000 kg initial mass, a power level of 60 kW, and a specific impulse of 2700 s.*

In the figure it is easy to see that the farther the moon is away from Jupiter, the longer it takes for Jupiter's gravitational pull to begin affecting the spacecraft. At the beginning of the trajectory the two-body and three-body cases are very similar. The two-body case has the radius continually gaining as the mass decreases, while the three-body case follows the same path, however the three-body radius oscillates around the value of the two-body case. The final few revolutions around the moon in the three-body case, is where the two-body and the three-body dynamics begin to differ drastically. In the final revolutions of the thee-body case, Jupiter's gravitational pull is beginning to overpower the gravitational pull of the moon; therefore the spacecraft's orbit is escaping from the moon at a much lower radius than dictated by two-body dynamics.

In order to use orbital averaging to estimate the mass and time for capture and escape trajectories, a cutoff point must be found at which to stop the algorithm. Figure 3.4 shows that if a proper cutoff radius in two-body dynamics can be selected, then the final mass calculated by orbital averaging will be a close approximation to the actual calculated three-body final mass. A logical cutoff parameter to use would be the L1 libration point. The L1 point is calculated in Eq. (2.19), and is the point at which a spacecraft goes from orbiting only one body to orbiting both bodies in a three-body system. The L1 libration point for Callisto is calculated to be 50,651 km away from the center of Callisto directly between the moon and Jupiter. This is 97.3 % of the way to Callisto from Jupiter, showing the massiveness of Jupiter compared to Callisto. Using the nominal case given above of initial mass of 2000 kg, power level of 60 kW and specific impulse of 2700 s, the final mass calculated using purely two-body dynamics is

1926 kg, the flight time is calculated to be 9.6 days. The final mass calculated using the L1 cutoff point for the same nominal case is 1933 kg, with a flight time of 8.7 days. The final mass using three-body dynamics is calculated in SNAP is 1934 kg with a flight time of 8.6 days. The difference in final mass has now decreased from 8 kg to only 1 kg, and the difference in flight time has decreased from 1 day to 0.1 days. However, using the L1 libration point as a cutoff doesn't work as well for the other Jovian moons. Table 3.2 presents the mass data, and Table 3.3 presents the time data for all four of the Galilean moons using the two-body, two-body with cutoff point of L1, and full three-body dynamics. All of the data is using the same initial conditions as above.

Table 3.2. *Mass data for all the Galilean moons using two-body, two-body with cutoff point of L1, and three-body dynamics with initial conditions of mass$_0$ 2000 kg, Power level 60 kW, specific impulse 2700 s.*

Moon	L1 pt (km)	3B Mass (kg)	2B L1 Mass (kg)	2B Mass (kg)
Io	10,642	1976.4	1960	1,921
Europa	13,744	1960.9	1958	1,939
Ganymede	32,000	1931.6	1937	1,917
Callisto	50,651	1934	1933	1,926

Table 3.3. *Transfer time data for all the Galilean moons using two-body, two-body with cutoff point of L1, and three-body dynamics with initial conditions of mass$_0$ 2000 kg, Power level 60 kW, specific impulse 2700 s.*

Moon	3B Time (days)	2B L1 Time (days)	2B Time (days)
Io	3.1	5.1	10.2
Europa	5.1	5.4	8
Ganymede	8.9	8.3	10.8
Callisto	8.6	8.7	9.6

Tables 3.2 and 3.3 clearly show that using the L1 libration point as a cutoff when using orbital averaging greatly improves the accuracy of the calculation. The two-body data for capturing into and escaping from Io is farther off from the actual three-body solution than any of the other moons. The lack of accuracy most likely occurs due to the fact that Io is located very deep inside of Jupiter's gravity well. While Io's L1 point is only 3,102 km less than Europa's, Io is about 250,000 km closer to Jupiter, which affects Jupiter's gravitational pull on the spacecraft drastically. Ganymede is the only moon that undershoots the time and mass calculations when using the L1 cutoff point compared to the three-body solution. The undershoot is probably due to the fact that Ganymede is the largest of the Galilean moons, and the gravitational pull that it applies to the spacecraft is greater than the pull that any of the other moons apply.

Although using the L1 libration point as a cutoff gives a reasonably accurate result, a more accurate method is desired. The next method attempted is using a different percentage of the L1 point for each individual moon. Figure 3.5 shows the trip time required for each Galilean moon using different percentages of the libration point as the cutoff variable for spacecraft with 2000 kg initial mass, a power level of 60 kW, and a specific impulse of 2700 s.

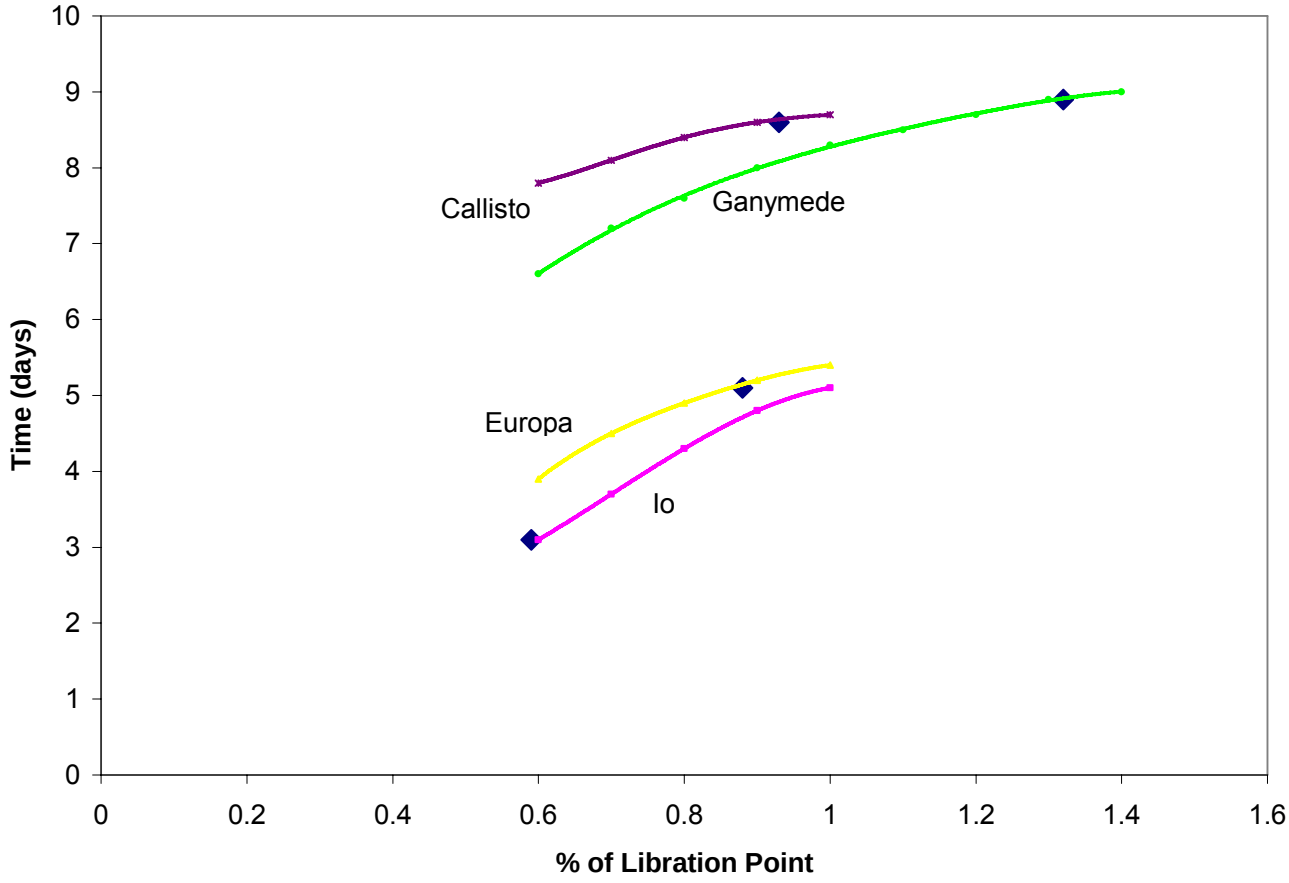

Fig. 3.5. *Trip time for each moon using the percentage of the L1 point as a cutoff variable for spacecraft with 2000 kg initial mass, a power level of 60 kW, and a specific impulse of 2700 s.*

Figure 3.5 shows that each of the different moons change with different rates when comparing what percentage of the libration point to use as a cutoff. The lines are the estimated values using the cutoff point method, and the large points on the lines are the actual times for each moon found using complete three-body dynamics. If a single libration point was going to be selected to be used for all of the moons, the standard L1 point would be the most central option. However at this particular thrust to weight ratio,

for accuracy to be maximized, Io should be cutoff at 60 % of the libration point, and Ganymede shouldn't be cutoff until 135 % of the L1 point.

Now that all of the properties of an orbit have been examined for a specific initial condition about each moon, the next step is to vary the initial condition. A single variable is desired to relate the input conditions to each other, therefore making it easier to compare each situation. Instead of continually changing the initial mass and thrust level, a variable that relates the two is used: thrust-to-weight ratio. The thrust-to-weight ratio is defined in Eq. (3.2).

$$\frac{T}{W} = \frac{T}{mg_0} = \frac{\dot{m}c}{mg_0} = \frac{\dot{m}I_{sp}}{m} \tag{3.2}$$

Where m is the current mass of the spacecraft and g_o is Earth's gravitational acceleration. The thrust-to-weight ratio increases with time due to the fuel mass decreasing which leads to a decreased current mass, assuming the spacecraft has a constant mass flow rate and specific impulse. However, for short trips using low thrust engines the thrust-to-weight can be considered constant. Figure 3.6 gives the data for a spacecraft escaping from Ganymede with a varying range of thrust-to-weight values.

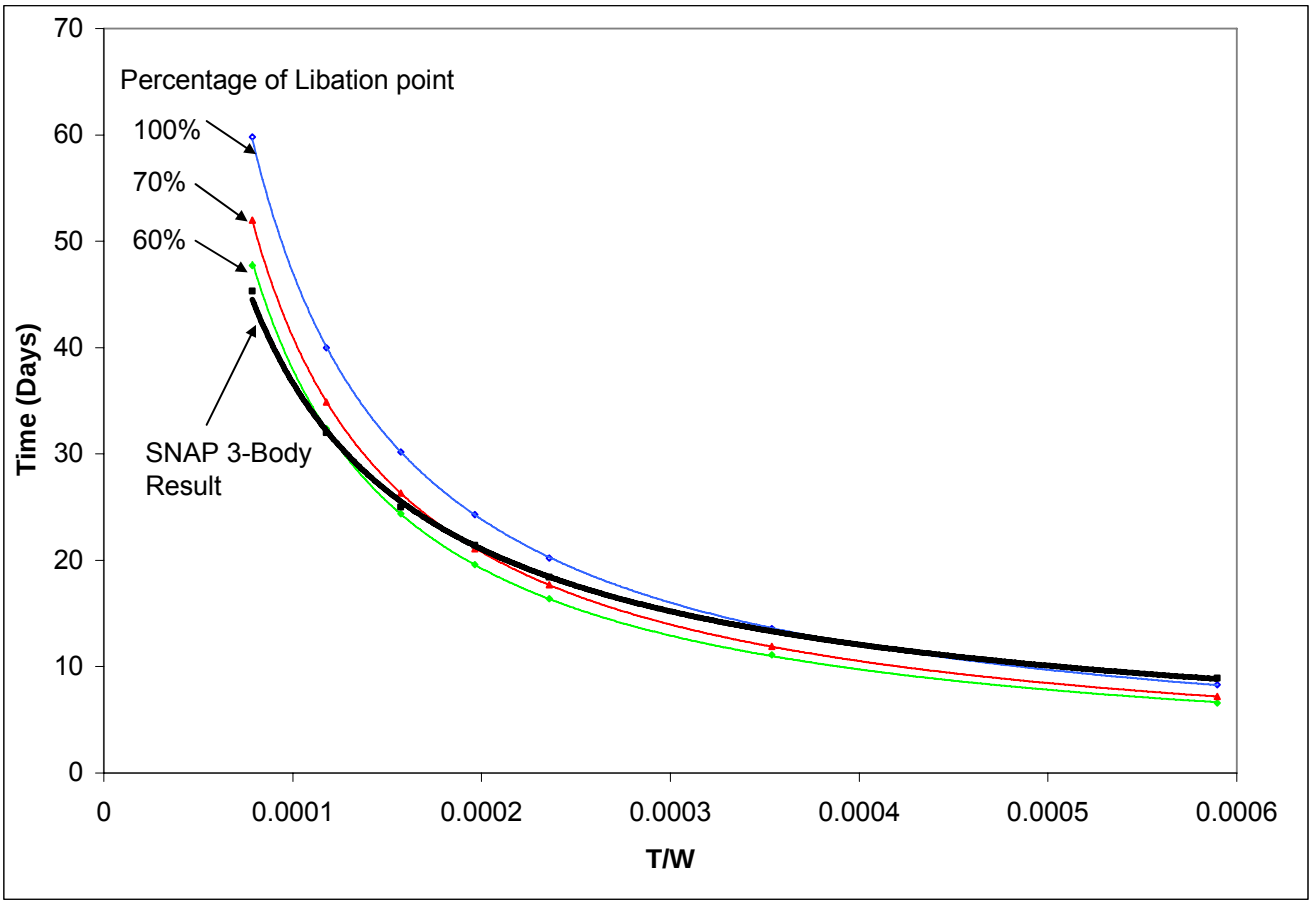

Fig. 3.6. *Trajectory data for spacecraft escaping Ganymede comparing varying thrust-to-weight ratios with escape time.*

Figure 3.6 shows that as the thrust-to-weight ratio is changed, the percentage of the libration point that a spacecraft reaches before it escapes also changes. There are four lines plotted on Fig. 3.6. The first is the actual 3-body solution found by using SNAP. The other three lines are the estimated values that orbital averaging gives when using 60 %, 70 %, and 100 % of the L1 point. At the higher thrust-to-weight ratios, a larger percentage of the libration point is needed for accurate calculation. In contrast, at lower thrust-to-weight ratios, a smaller percentage of the libration point is needed. Figure 3.6

clearly shows however that a single cutoff value can not be used for each moon, and that a more in depth solution must be sought.

Table 3.4 is a table of the capture and escape data made by running SNAP for all feasible ranges of the thrust-to-weight ratio for each of the Galilean moons. This table shows the time to escape to zero energy for every initial condition that a spacecraft using electric propulsion might have.

Table 3.4. *Escape time for a spacecraft orbiting each of the Galilean moons with varying thrust-to-weight ratios.*

Time to Escape to Zero Energy (Days)				
T/W	Io	Europa	Ganymede	Callisto
0.0001	*	37.3	69.3	88.5
0.0002	*	21.9	37.7	48.5
0.0003	7.4	15	27.3	33.7
0.0004	7	10.9	21	26.6
0.0005	5.8	9.9	18	21.3
0.0008	3.8	7	12.7	15
0.001	3.3	5.7	9.9	9.9
0.0025	1.7	3	4	4
0.005	1.2	2.6	2	2
0.01	0.8	1.5	1	0.9

The initial condition for all the spacecrafts in Table 3.3 is that the spacecrafts are in a circular, planar orbit about their respective moons with a radius of one moon radii. The time a spacecraft takes to reach zero energy when related to the thrust-to-weight ratio, has a logarithmic look to it. Figure 3.7 shows this by plotting the thrust-to-weight ratio with respect to the time; also a logarithmic trend line has been plotted over the points to show the relationship that the thrust-to-weight ratio has with trip time.

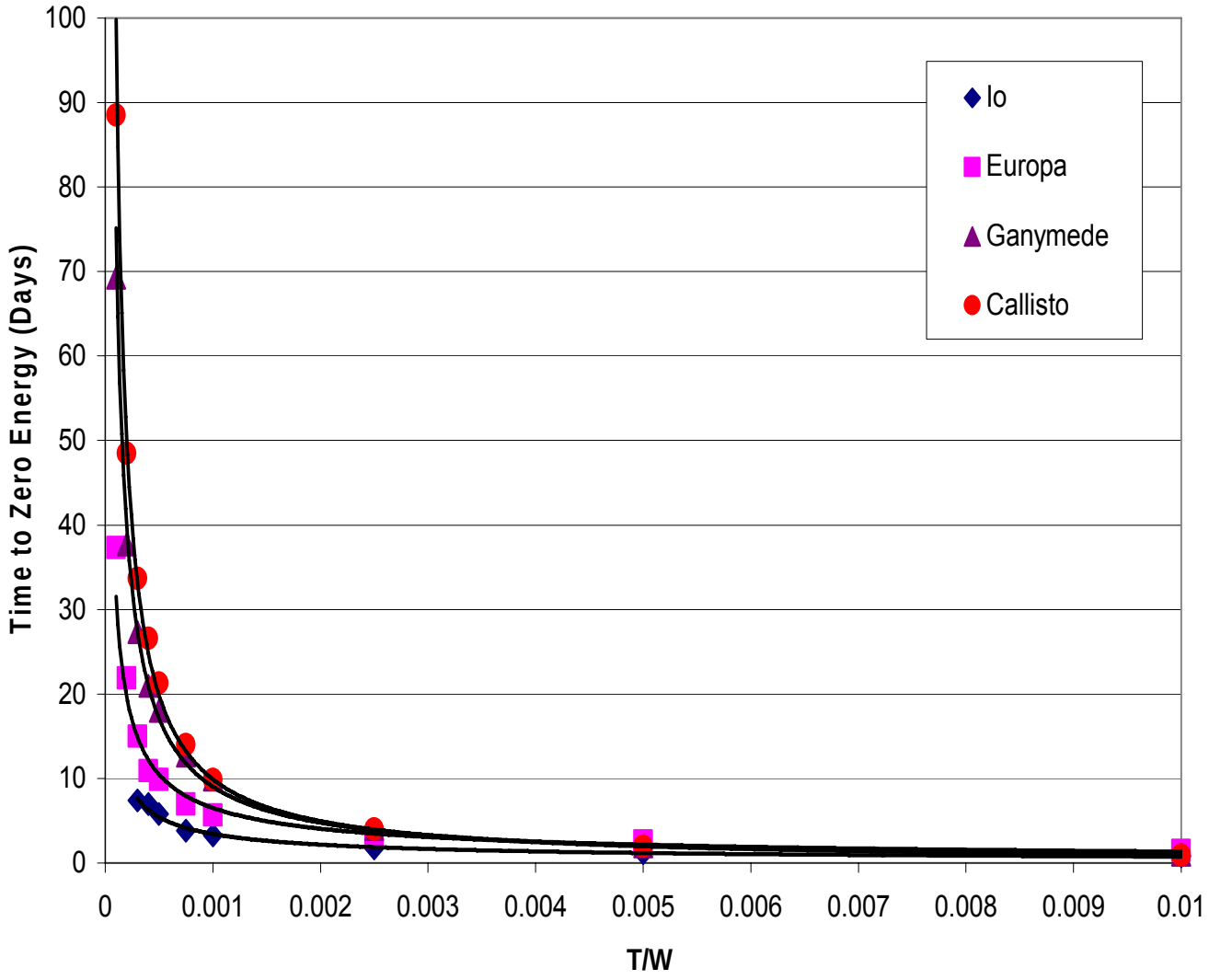

Fig. 3.7. *Escape time for a spacecraft orbiting each of the Galilean moons with varying thrust-to-weight ratios found using SNAP.*

The time that a spacecraft takes to escape each moon increases as the thrust-to-weight ratio decreases. As expected, the closer proximity to Jupiter the moon has the quicker the spacecraft escapes from the moon's orbit. As the thrust-to-weight ratio decreases below 0.001 the time to escape increases drastically for the three farthest moons.

In Table 3.3 Io does not have a value for the two lowest thrust-to-weight ratios because a spacecraft with that little thrust cannot escape Io's gravity field without Jupiter perturbing the spacecraft enough to cause the spacecraft to crash into Io's surface. Even for the higher thrust-to-weight ratios, when using purely tangential steering, a spacecraft escaping Io must be in a proper orientation with Jupiter which allows the spacecraft to escape without impacting the body. Io is not the only moon that requires the spacecraft to be in a certain orientation with respect to Jupiter to avoid crashing; Europa requires an orientation examination also.

Increasing the Radius of Periapsis

In order to check what orientations a spacecraft is capable of launching from to be able to escape without impact, numerical integration must be used. Since the orbital element that must be tracked is the true anomaly, orbital averaging cannot be used because that is the one orbital element that orbital averaging loses in the process. A MATLAB code has been developed that uses three-body dynamics to calculate the escape of a spacecraft from a moon in the Jovian system. The code uses the relative acceleration approach described in section 2.1.2, which is a three-body dynamics approach. In order to battle the problem of the spacecraft crashing into the moon on escape, a new steering law is developed that constantly thrusts to increase the radius of periapsis instead of purely thrusting along the velocity vector.

The MATLAB code developed is tested against SNAP to show that the code is correct. An escape trajectory for a spacecraft with the same initial conditions is run in

both SNAP and MATLAB. These initial conditions are: a power level of 20 kW, a specific impulse of 2700 s, and an initial mass of 1000 kg. The spacecraft starts in a 2-Europa radii circular orbit, and the spacecraft leads Jupiter with an angular separation of 8.5 degrees. The spacecraft is then propagated to escape. Figure 3.8 shows the energy of each orbit as it propagates.

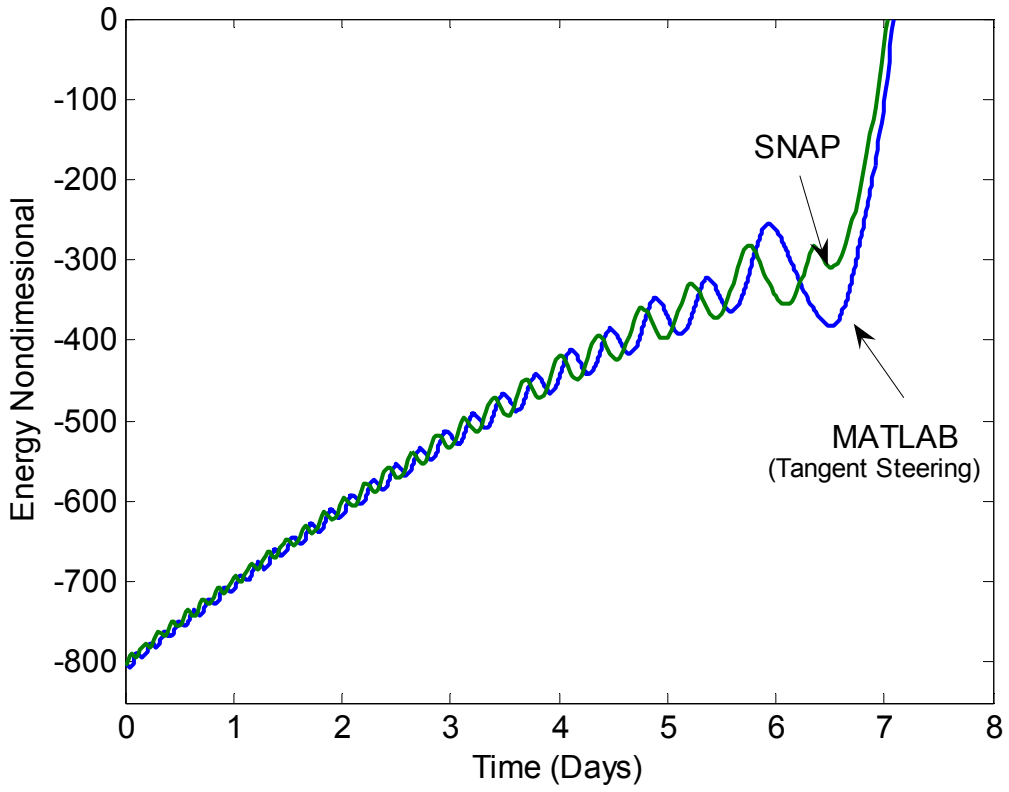

Fig. 3.8. *Energy of 2 Europa radii circular orbits propagated to escape for both MATLAB and SNAP runs using tangential steering with a spacecraft with 20 kW power, 1000 kg mass, and 2700 s specific impulse.*

The energies of the orbits match each other closely. The reasons for the slight differences in the energies are due to a few approximations that are made. The first approximation that is made is that the Jupiter-moon system is a two-dimensional system.

The moon actually has about a half of a degree of inclination with respect to Jupiter. The second approximation that is made is that there are no planet gravity harmonics, when actually Jupiter does have harmonics. Even with these approximations though the energies of the orbits closely match each other which shows that the MATLAB code properly propagates the orbit of a spacecraft.

When the spacecraft uses tangential steering the spacecraft sometime crashes into the moon on the final escape revolution because of Jupiter's gravitational pull. The first step for calculating an orbit of a spacecraft that needs to increase the radius periapsis is to find the proper steering angle in which the spacecraft should thrust. In order to find this angle, the derivative of the radius of periapsis equation must be taken. The radius of periapsis equation is given in Eq. (2.7), and its derivative is

$$\dot{r}_p = \dot{a}(1-\varepsilon) - \dot{\varepsilon}a \tag{3.3}$$

The only variables in the equation are the semimajor axis, eccentricity, and their respective derivatives. Now equations for the rate of change of the semimajor axis and eccentricity are given in Eqs. (3.3)-(3.4).

$$\dot{a} = \frac{2a^2\varepsilon\sin\nu}{h}T\sin\alpha + \frac{2a^2 p}{hr}T\cos\alpha \tag{3.4}$$

$$\dot{\varepsilon} = \frac{1}{h}p\sin\nu\, T\sin\alpha + \frac{1}{h}[(p+r)\cos\nu + r\varepsilon]T\cos\alpha \tag{3.5}$$

In these equations T is the thrust, α is the thrust steering angle with respect to the local horizon, and a, ε, υ, h, p, and r are orbital elements or properties described in Section 2. The next step requires taking Eq. (3.3) substituting in Eqs. (3.4) and (3.5) and taking the derivative with respect to the steering angle. The reason that the derivate is taken is because the α desired is the α that maximizes $\dot{r}_p$, and this occurs when $\partial r_p/\partial\alpha=0$. When

all of these steps are taken an equation for the steering angle is developed, Eq. (3.6), with a little rearranging of variables.

(3.6)

$$\alpha = -\tan^{-1}\left(\frac{r\sin\upsilon a\left(-2\varepsilon+\varepsilon^2+1\right)}{2a^2-2a^2\varepsilon-2a^2\varepsilon^2+2a^2\varepsilon^3-r\cos\upsilon a+r\cos\upsilon a\varepsilon^2-r^2\cos\upsilon-r^2\varepsilon}\right)$$

The steering angle can be calculated now, however in order to use the relative acceleration approach, the unit vectors for the thrust must be in Cartesian coordinates. The best way to convert the steering angle to Cartesian coordinates is to find the relationship between the steering angle and the velocity vector. In order to do this the steering angle is simply subtracted from the flight-path angle calculated in Eq. (2.11). Once this new steering angle has been found, the unit vectors in the standard Cartesian coordinate system can be calculated using Eqs. (3.7) and (3.8).

$$u_x = \cos\left(\tan^{-1}\left(\frac{v_y}{v_x}\right)-\alpha_v\right) \tag{3.7}$$

$$u_y = \sin\left(\tan^{-1}\left(\frac{v_y}{v_x}\right)-\alpha_v\right) \tag{3.8}$$

In these equations α_v is the steering angle with respect to the velocity. Now that the unit vectors for the direction of the thrust have been calculated, they need to be turned into accelerations. This is done simply by dividing the thrust by the mass.

$$\vec{a}_t = \frac{T}{m}\hat{u} \tag{3.9}$$

$$\hat{u} = \begin{bmatrix} u_x \\ u_y \end{bmatrix} \tag{3.10}$$

This acceleration value now can be added to Eq. (2.28). This gives the equations of motion of the spacecraft; the vector form of the equations is given in Eq. (3.9).

$$\ddot{\vec{\rho}}_{13} = -\frac{Gm_1}{\rho_{13}^{\ 3}}\vec{\rho}_{13} - \frac{Gm_2}{\rho_{23}^{\ 3}}\vec{\rho}_{23} - \frac{Gm_2}{\rho_{12}^{\ 3}}\vec{\rho}_{12} + \vec{a}_T \tag{3.9}$$

Where a_T is the acceleration due to thrust. Integrating Eq. (3.9) propagates the orbit of a spacecraft.

Now that the new steering law has been developed, it must be tested. In order to test the new steering law, a nominal case in which the spacecraft crashes into the surface of the moon is examined. The nominal case is for a spacecraft with 35 kW of power starting in a circular trajectory of three moon radii about Europa. The spacecraft starts aligned with Jupiter along the x axis. Figure 3.9 gives both the new periapsis gain steering law and tangential steering on the same plot with respect to the velocity vector for the entire trip time. Figure 3.10 shows a sample of the periapsis gain steering law angle for one revolution of an orbit with respect to true anomaly. The sample orbit chosen for Fig. 3.10 is an orbit with 0.333 eccentricity and a semimajor axis of 4 Europa radii.

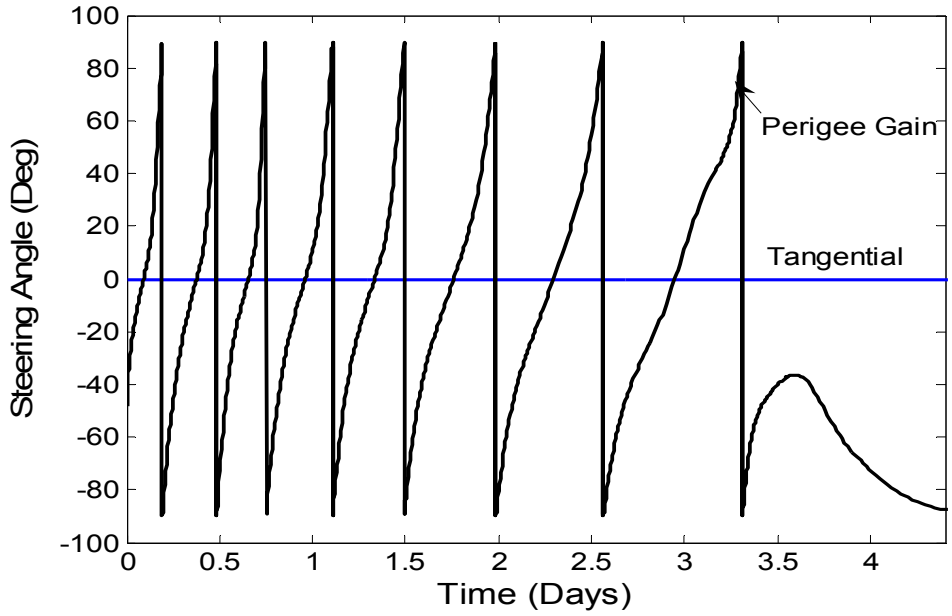

Fig. 3.9. *Tangential and periapsis gain steering laws plotted for a spacecraft escaping a three radii circle about Europa with 35 kW thrust and 1000 kg initial mass.*

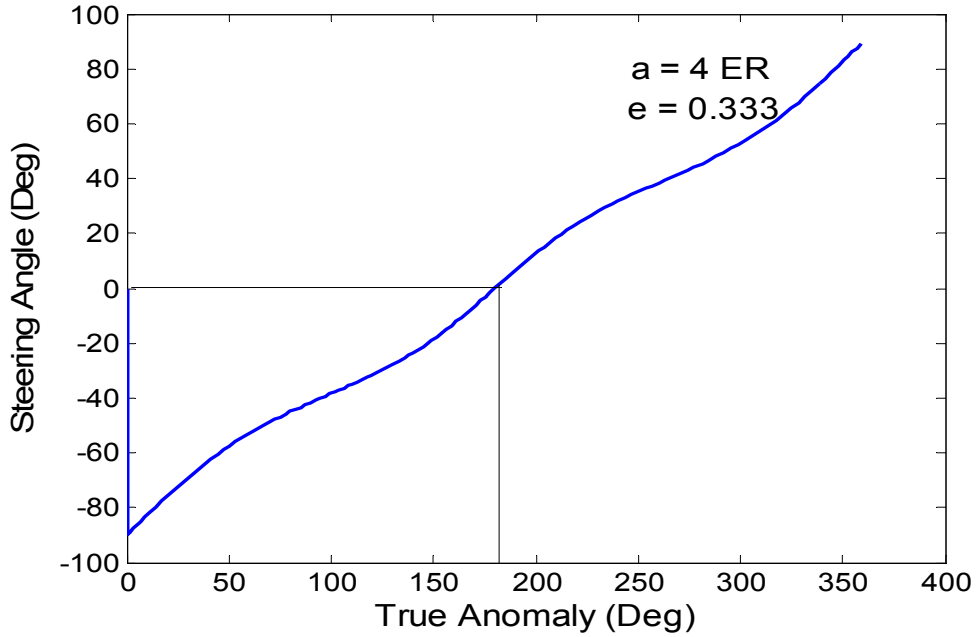

Fig. 3.10. *Periapsis gain steering law plotted with respect to true anomaly for a spacecraft escaping a three radii circle about Europa with 35 kW thrust and 1000 kg initial mass.*

The true anomaly of the spacecraft is also plotted for the new steering law. The steering angle continually revolves from -90 deg to 90 deg. At apoapsis, when the true anomaly = 180 deg, the thrust is pointing directly in the direction of the velocity, $\alpha = 0$. The figure shows that when the spacecraft is near apoapsis tangential steering increases periapsis at the maximum rate. As the spacecraft advances to where it is halfway between apogee and periapsis, the thrust angle is slowly increasing from the velocity vector. When the spacecraft arrives at periapsis the thrust angle has increased to 90 deg from the velocity pointing directly away from the moon. When the spacecraft gets just past periapsis the thrust swings 180 deg and points directly towards the moon. Figure 3.11 shows a schematic of what the thrust vector looks like over the course of one revolution of an orbit.

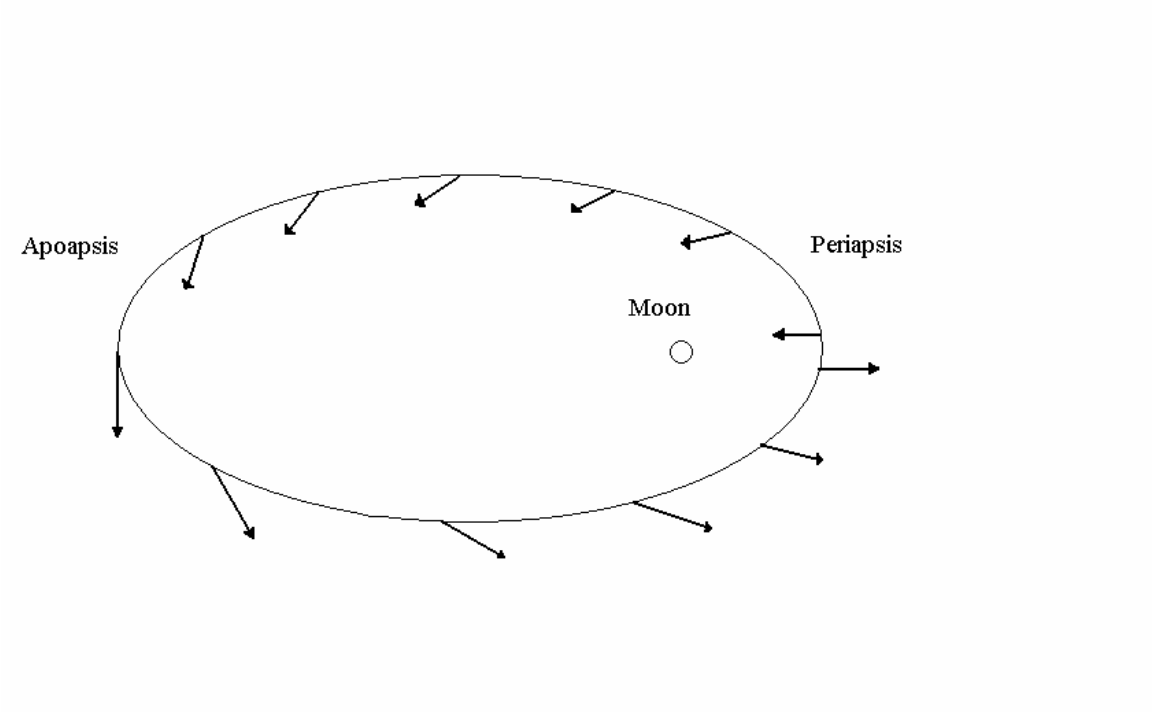

Fig. 3.11. *Thrust vector direction for periapsis gain steering law.*

The figure only shows a representative direction, the exact angle that the thrusters are pointing must be found in Fig. 3.10.

The actual trajectories are shown in Figure 3.12; both the tangentially thrusting trajectory, as well as the trajectory thrusting along the steering angle.

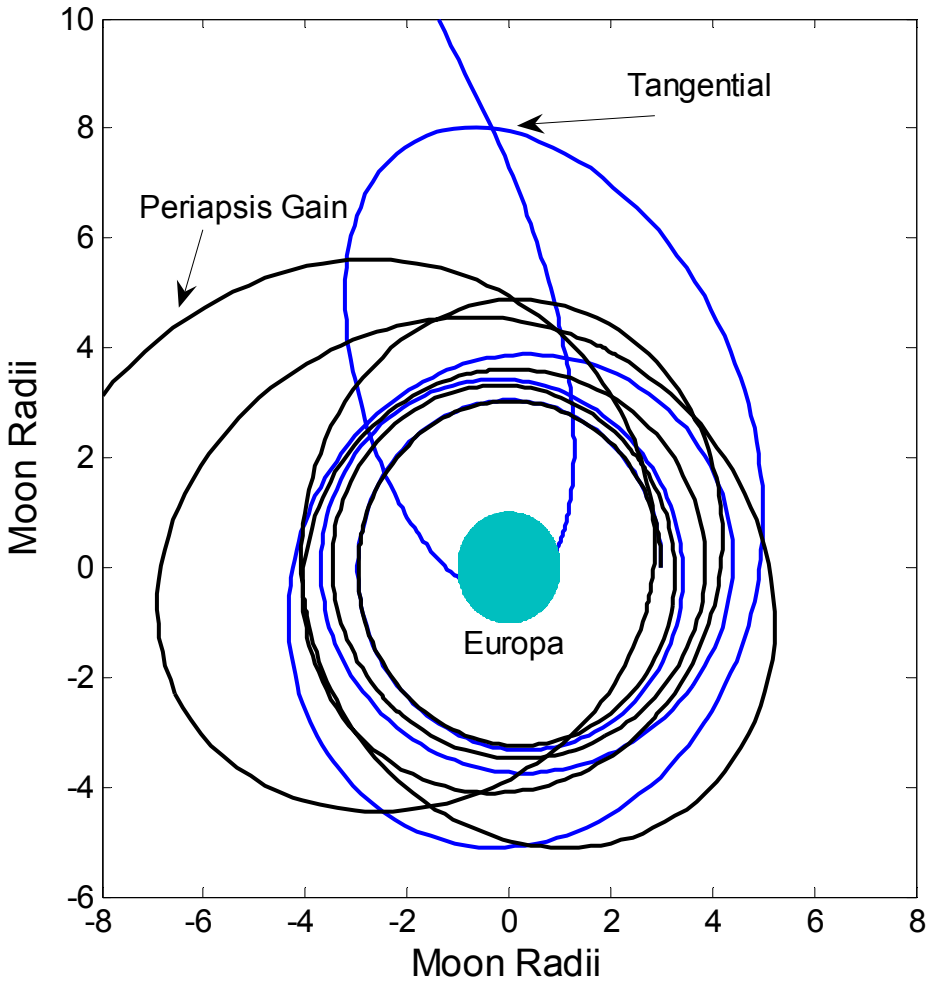

Fig. 3.12. *Trajectories for tangential and periapsis gain steering laws for a spacecraft escaping a three radii circle about Europa with 35 kW thrust and 1000 kg initial mass.*

The tangential steering trajectory crashes into Europa on its last pass of the moon before escape due to the pull on the spacecraft by Jupiter. Using the periapsis gain steering law however, the radius of periapsis is increased which allows the spacecraft to escape without crashing into Jupiter. The radius of periapsis is clearly increasing drastically in the periapsis gain steering trajectory. To better illustrate this, Fig. 3.13 shows the radius of periapsis for both trajectories at all times during the orbit.

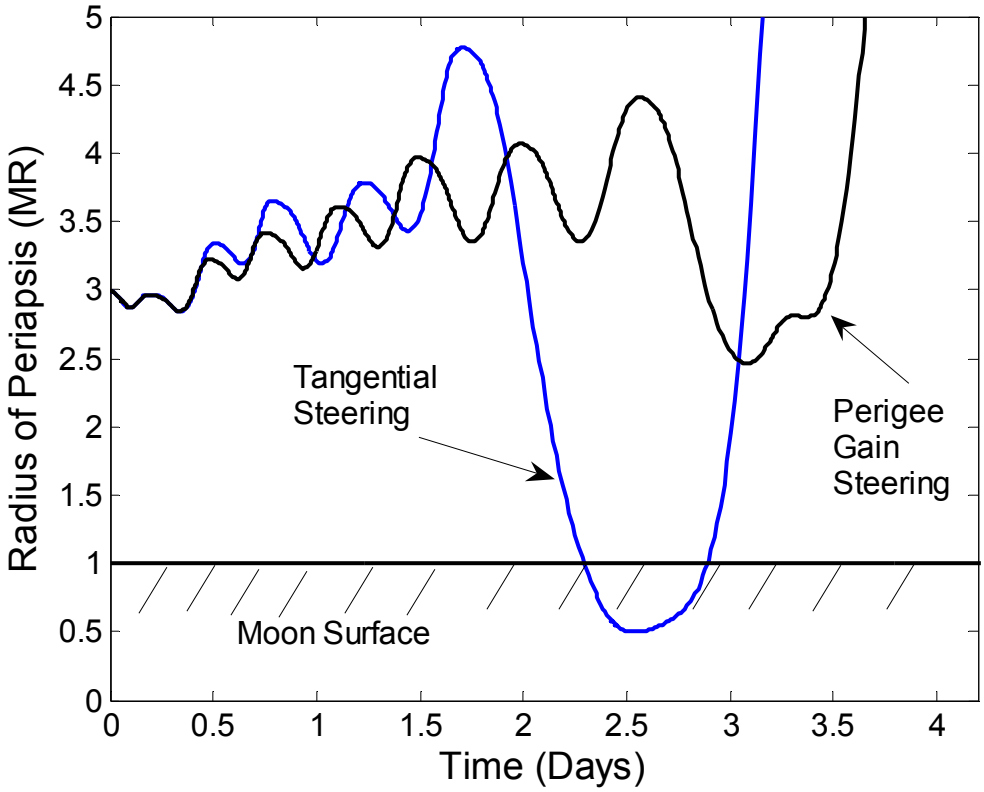

Fig. 3.13. *Radius of periapsis for both tangential and periapsis gain steering for a spacecraft escaping a three radii circle about Europa with 35 kW thrust and 1000 kg initial mass.*

The periapsis gain steering does not always have a higher radius of periapsis than tangential steering. One reason for this is because the radius of periapsis derivation was

for a two-body situation. The pull of Jupiter on the spacecraft is affecting the radius of periapsis in the three-body case. Another reason that the functions look different is because due to the different steering laws, the orbits are different. However, the periapsis gain steering does keep the spacecraft from coming dangerously close to impacting the planet's surface because the radius of periapsis consistently increases and doesn't dip below the moon's surface like the tangential steering law. The periapsis gain steering does however add time to the trip. Figure 3.14 shows the energy of the spacecraft for each of the steering laws over the entire trip.

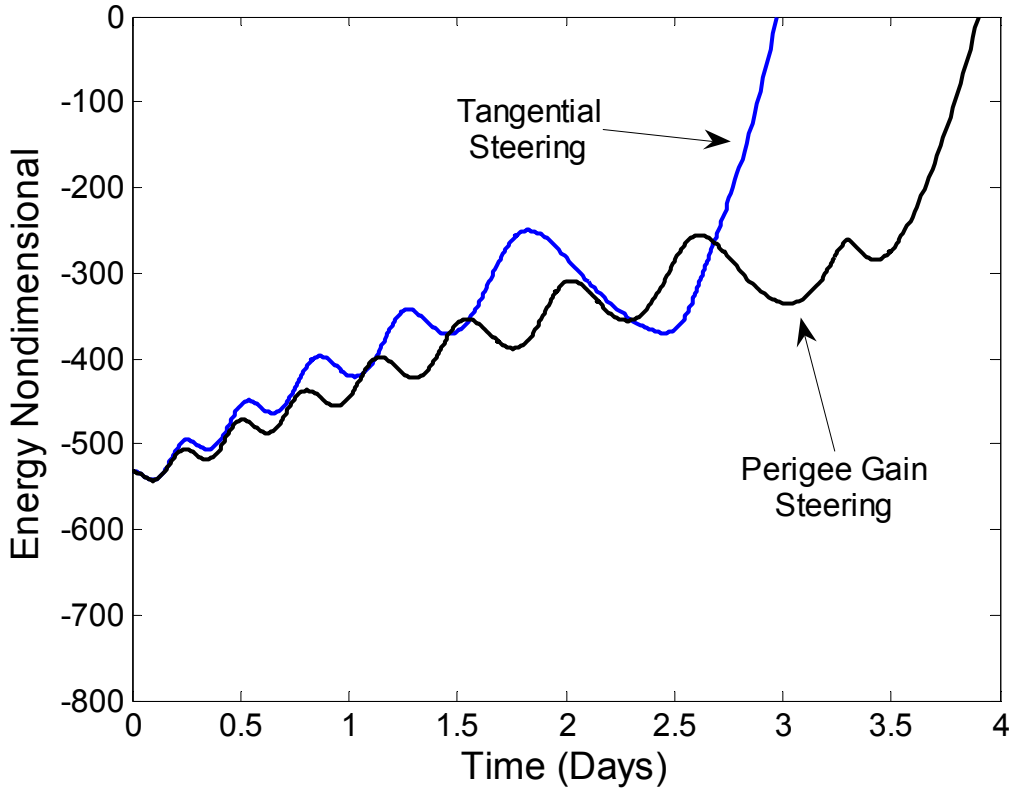

Fig. 3.14. *Energy of tangential and periapsis gain steering laws for a spacecraft escaping a three radii circle about Europa with 35 kW thrust and 1000 kg initial mass.*

A spacecraft escapes from a body when the energy of its orbit reaches zero. Therefore, Fig. 3.14 shows that the tangential steering law escapes around an entire day before the periapsis gain steering law does. There are now two steering laws that each have there benefits. The tangential steering law escapes in the minimum time because it maximizes the power since the force and velocity vectors are aligned; however it impacts the surface of the moon. The periapsis gain steering law takes longer to escape, but it fixes the problem of collision with the moon by increasing the radius of periapsis. Next an attempt to combine the two steering laws will be made in order to take advantage of both of there benefits.

In order to combine the two steering laws, a limiter is placed in the system. The steering angle with respect to the velocity vector is limited to a value less than 90 deg. The limiter is due to the fact that if the steering angle is 90 deg then there is no energy gain because $\vec{T} \cdot \vec{V} = 0$. Limiting this angle will help the spacecraft increase energy better when the spacecraft is near periapsis in the orbit. Figure 3.15 shows a block diagram of how the system works.

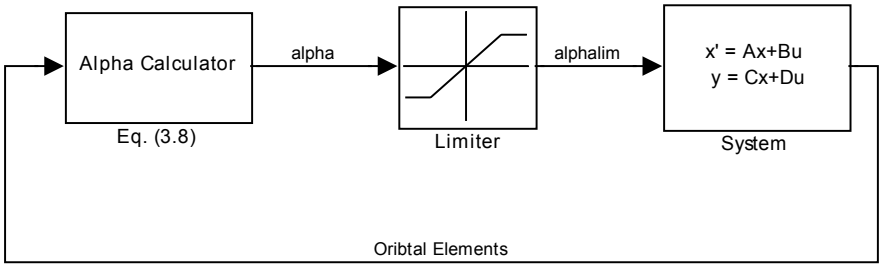

Fig. 3.15. *Block diagram of system that limits the steering angle.*

Limiting the steering angle does not affect the periapsis gain steering law when the spacecraft is near apogee. This is because the steering angle is at or near zero, tangent steering, when the spacecraft is near apogee; however when the spacecraft begins to approach periapsis the limiter goes into effect and limits the steering angle. The same nominal case as above is considered for these calculations. This way the difference between the unlimited periapsis gain steering law and the limited steering law can be easily compared. Four limiting values were considered: 10, 20, 30, and 40 deg. The reason these values are chosen is that if the angle gets any greater than this the spacecraft is not thrusting to help itself escape from the moon when it is near periapsis. When discussing the following graphs, they will be considered as subplots a, b, c, and d which will be orientated upper left, upper right, lower left, and lower right respectively. The graphs will also start with a being the 40 deg limiter and decreasing in value until d is the

10 deg limiter. Figure 3.16 shows the steering angle for the trip time for each of the limiters examined.

a) b)

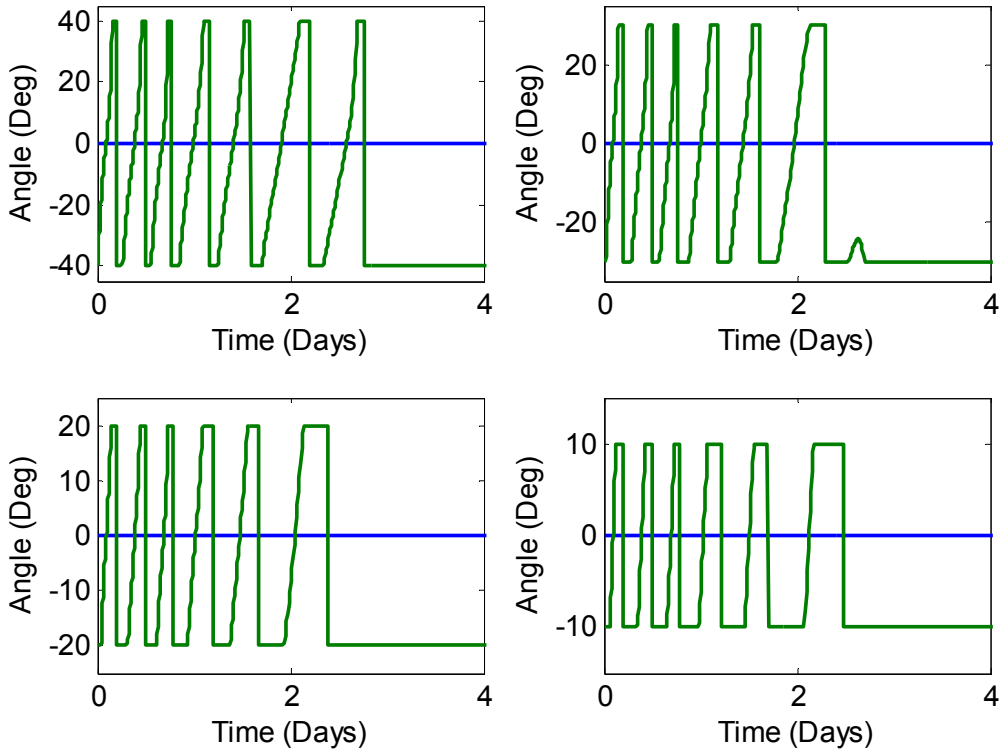

c) d)

Fig. 3.16. *Tangential and limited periapsis gain steering laws, a) 40 deg, b) 30 deg, c) 20 deg, d) 10 deg, plotted for a spacecraft escaping a three radii circle about Europa with 35 kW thrust and 1000 kg initial mass.*

All of the limited scenarios appear similar to the unlimited case between the limits. It can easily be seen that as the limiter decreases in value the amount of time that the spacecraft thrusts at the limit increases. The limiter affects the trajectory of the orbit as well. The trajectories of each of the limited values are given in Fig. 3.17.

a) b)

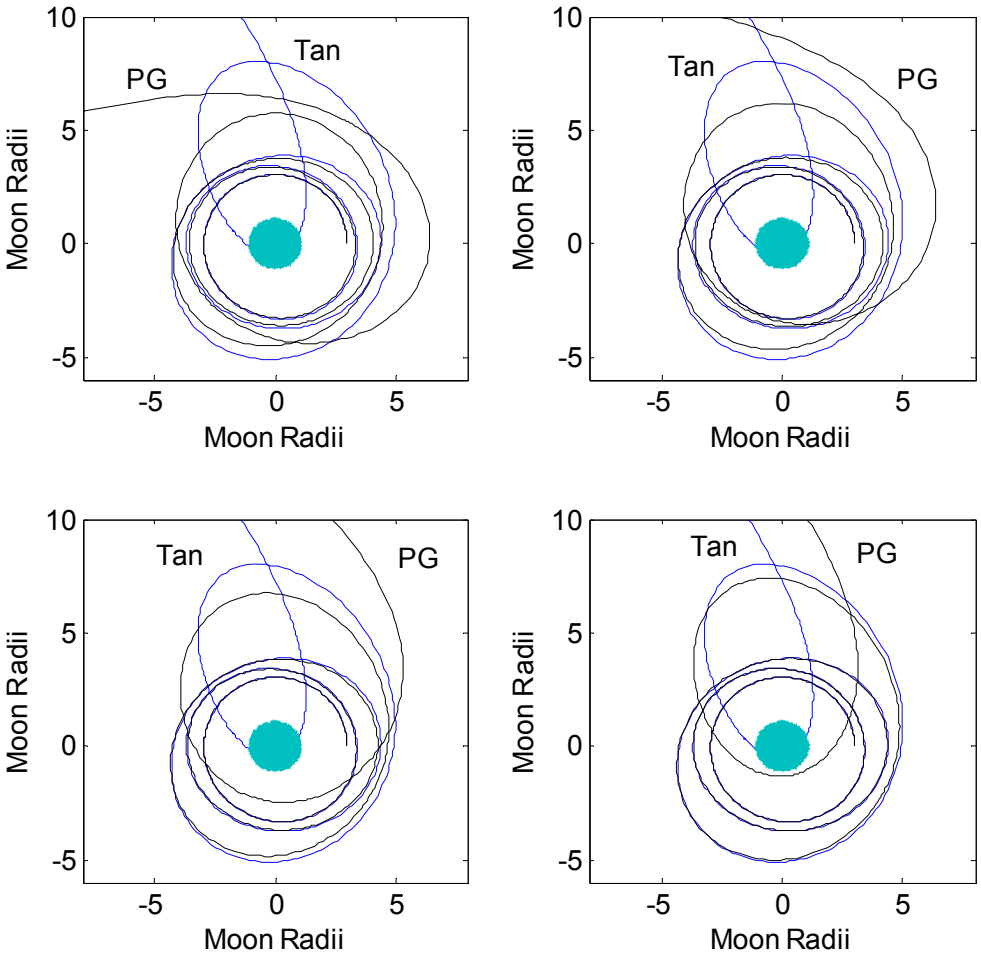

c) d)

Fig. 3.17. *Trajectories for tangential and limited periapsis gain steering laws, a) 40 deg, b) 30 deg, c) 20 deg, d) 10 deg, plotted for a spacecraft escaping a three radii circle about Europa with 35 kW thrust and 1000 kg initial mass.*

Figure 3.17 shows that as the value for the limiter decreases, the orbit that the limited periapsis gain steering law provides begins looking more and more like the

tangential steering trajectory. The amount of energy that is being added to the orbit is greatest in the 10 deg limiter. This can be seen by viewing how the spacecraft escapes from the moon. The 10 deg limiter escapes very similarly to tangential steering, minimum time, while when the 40 deg limiter is examined, an entire extra revolution is need before escape occurs. Figure 3.18 show the radius of periapsis for each limiter so that the distance can be compared with tangential steering.

a) b)

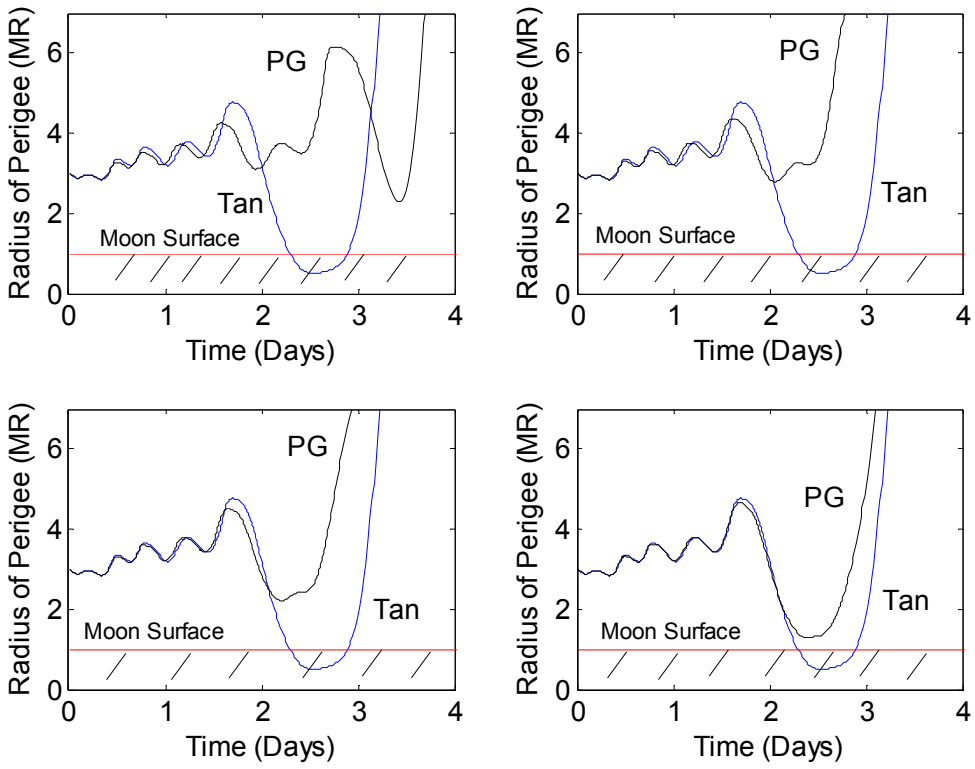

c) d)

Fig. 3.18. *Radius of periapsis for tangential and limited periapsis gain steering laws, a) 40 deg, b) 30 deg, c) 20 deg, d) 10 deg, plotted for a spacecraft escaping a three radii circle about Europa with 35 kW thrust and 1000 kg initial mass.*

The 10, 20, and 30 deg limiter radius of periapsis plots look very similar to the tangential steering plots with exception to the last revolution where the tangential plot dips below the moon's surface and crashes and the periapsis gain steering helps limit the dip that Jupiter's gravitational pull causes. The greater the value of the limiter, the greater the radius of periapsis is in the end. The reason the 40 deg limiter has the extra dip in the radius of periapsis is because of the tradeoff between periapsis gain and energy addition. The 40 deg orbit requires an extra revolution to escape and Jupiter's gravitational pull causes the extra dip in the radius of periapsis. Figure 3.19 presents the energies of the orbits with each limiter.

a) b)

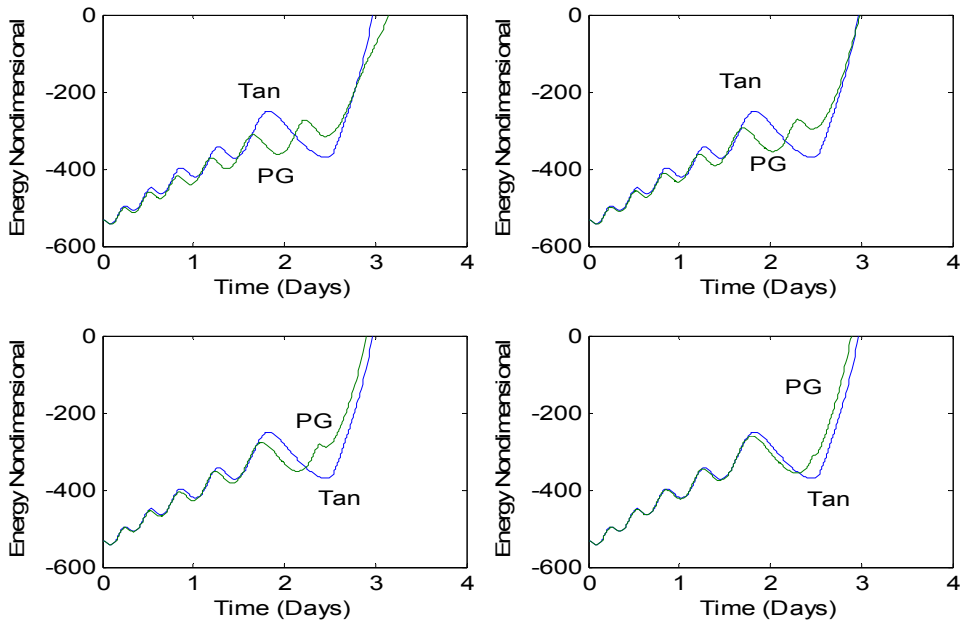

c) d)

Fig. 3.19. *Nondimensional energy for tangential and limited periapsis gain steering laws, a) 40 deg, b) 30 deg, c) 20 deg, d) 10 deg, plotted for a spacecraft escaping a three radii circle about Europa with 35 kW thrust and 1000 kg initial mass.*

Each of the limiter values has a similar escape time to that of tangent steering. The 40 deg limiter takes slightly longer than the others due to the extra revolution required. The data gathered from the graphs discussing the limiter shows that using the periapsis gain steering with a limiter is an adequate solution to for finding a feasible escape trajectory from the Galilean moons.

Transfers between Moons

Once the spacecraft has departed the first moon or any subsequent moon thereafter, the next phase of the trajectory is for the spacecraft to rendezvous with the next desired moon. In order for the spacecraft to rendezvous with the following moon many revolutions about Jupiter are required. Due to the large number of revolutions, the computational load of integration is large. Therefore, approximating the solution with an analytic estimation for the time and mass spent in this phase of the trajectory is desirable. The condition of the spacecraft when it escapes the initial moon with respect to Jupiter is that the spacecraft is in a circular, planar orbit about Jupiter with a radius of the magnitude of the semimajor axis of the moon that the spacecraft has just escaped. The desired final condition of the spacecraft is that the spacecraft will be in a circular, planar orbit about Jupiter with a radius of the magnitude of the semimajor axis of the receiving moon. Edelbaum's equation, Eq. (2.54), calculates the time necessary for a spacecraft to transfer from one circular orbit to another. This completely satisfies the needs of the spacecraft. Table 3.5 gives the data for integrated trajectories, as well as the data for

Edelbaum's equation for transfers between all of the Galilean moons. The spacecraft has the initial conditions of mass 2000 kg, thruster level 10 kW, specific impulse 2700 s.

Table 3.5 *Data comparing the difference in mass between numerical integration and Edelbaum's equation for a spacecraft with initial conditions of 2000 kg mass, 10 kW power, and 2700 s specific impulse.*

Moon Transfer	Δ V (km/s)		Δ Mass (%)
	Integration	Edelbaum	
Callisto-Ganymede	2.718149	2.68049	0.1422207
Callisto-Europa	5.661164	5.546173	0.4336401
Callisto-Io	9.266721	9.138866	0.4820339
Ganymede-Europa	2.895517	2.865683	0.1126882
Ganymede-Io	6.516755	6.458376	0.2203889
Europa-Io	3.614148	3.592693	0.0810526

The ΔV values for Edelbaum's equation are similar to those found by using integration. The Δ Mass %, or final mass error, is calculated between Edelbaum's equation and integration is always less than a half of a percent. This allows the use of Edelbaum's equation when calculating the time of flight and mass for transfers between the Galilean moons.

Complete Moon Tour

Now that a spacecraft can be captured by Jupiter, captured into each Galilean moon, escape each moon's sphere of influence, and transfer between each moon, the final mass and total trip time of an entire Jupiter moon tour can be calculated for different initial

conditions. A complete tour of Jupiter's moons includes: capturing into Callisto from a parabolic entry orbit at Jupiter's sphere of influence, capturing into and escaping from Callisto, transferring from Callisto's orbit to Ganymede's orbit, capturing into and escaping from Ganymede, transferring from Ganymede's orbit to Europa's orbit, capturing into and escaping from Europa, transferring from Europa's orbit to Io's orbit, and capture into Io. The spacecraft is not required to return to Earth, therefore once the spacecraft has visited the final moon the tour is complete. The spacecraft will then remain at the final destination until Jupiter's radiation destroys the equipment. Table 3.6 gives the mass and trip time for a spacecraft to complete the entire moon tour.

Table 3.6. *Mass and time of flight for spacecraft completing entire Jupiter moon tour with a specific impulse of 2700 s and efficiency of 0.49.*

$Mass_0$ (kg)	P_O (kW)	$Mass_f$ (kg)	Time (Yrs)	T/W
1000	10	420.07	1.62	7.61E-04
1000	20	410.50	0.82	1.53E-03
2000	10	849.68	3.21	3.78E-04
2000	20	840.14	1.62	7.61E-04
3000	10	1247.12	4.90	2.59E-04
3000	20	1264.40	2.42	5.07E-04
5000	10	2126.57	8.03	1.52E-04
5000	20	1966.40	3.23	1.57E-04

All of the entries in Table 3.5 have a specific impulse of 2700 s and an efficiency of 0.49. The thrust-to-weight ratio listed in the table is the thrust-to-weight ratio at the end of the trajectory. The ratio varies over the entire trajectory according to the current mass of the spacecraft. The time of flight of the trajectory increases as the mass of the spacecraft increases assuming the power level remains the same. When holding the initial mass of the spacecraft constant and doubling the power level the flight time is nearly cut in half.

The final mass also drops a small amount. Just looking at final mass numbers the higher power level would always be chosen because of the slim difference in final mass compared to the drastic difference in flight time; however the additional mass of the propulsion system due to the greater power level is not being taken into consideration when purely comparing final masses. When the trip times are computed, there is no added trip time for stays at each moon in order for science calculations. The final mass values in Table 3.5 are sufficient for only very minimal amounts of science to be taken at the moons for two reasons. First the final mass allows for only a small amount of science equipment due to weight restrictions. Secondly, also due to weight restrictions only a small amount of radiation shielding can be added onto the spacecraft. With only a small amount of radiation shielding the life of the spacecraft's science devices is also small. Depending on the amount of science that the scientists desire, as well as the desired cost of the mission, a spacecraft with larger initial mass might be required. Therefore Table 3.7 gives data for a spacecraft completing an entire moon tour with higher initial masses.

Table 3.7. *Mass and time of flight for spacecraft completing entire Jupiter moon tour with a specific impulse of 7000 s and efficiency of 0.70.*

$Mass_0$ (kg)	P_O (kW)	$Mass_f$ (kg)	Time (Yrs)	T/W
10000	50	6639.35	7.15	1.51E-04
10000	100	6506.40	3.72	3.07E-04
20000	60	13276.97	11.93	9.05E-05
20000	100	13080.36	7.37	1.51E-04
30000	50	19905.80	21.49	5.05E-05
30000	100	19861.15	10.79	1.01E-04

For Table 3.7 the specific impulse and efficiency of the spacecraft have also been increased to 7000 s and 0.70 respectively in order to provide better fuel consumption due

to the higher power levels of the thrusters. The times of the transfers have increased drastically, however the final masses have also increased proportionally. The increase in final mass allows for much more science data to be gathered by the spacecrafts because the amount of science equipment can be increased, as well as the radiation shielding can also be increased.

CHAPTER 4 SUMMARY AND CONCLUSIONS

A spacecraft using low-thrust propulsion can perform a complete tour of the Galilean moons. Simple analytical methods assuming two-body tangent steering can be used to calculate trip time and fuel mass when the spacecraft is away from the moons in Jupiter space. When the spacecraft captures into and escapes from the moons however three-body integration is required.

In order to complete a Galilean moon tour, these steps must be performed in a sequential order: capturing into Callisto from a parabolic entry orbit at Jupiter's sphere of influence, capturing into and escaping from Callisto, transferring from Callisto's orbit to Ganymede's orbit, capturing into and escaping from Ganymede, transferring from Ganymede's orbit to Europa's orbit, capturing into and escaping from Europa, transferring from Europa's orbit to Io's orbit, and capture into Io. Once the first step has been completed, the final values from it are taken as the initial values for the next step. This process is repeated until there are no steps remaining.

The spacecraft starts in a parabolic orbit at Jupiter's sphere of influence. Orbital averaging is used to decrease the energy of the orbit until the spacecraft reaches Callisto. The orbital averaging method matches integration well; this comparison is shown in reference 27. Depending on the thrust-to-weight ratio the time to reach Callisto can vary from a few months to several years.

There were several methods tried for calculating the trip time and final mass of the spacecraft when capturing into and escaping from the moons: two-body dynamics, two-body dynamics using the L1 point as a cutoff, two-body dynamics using a percentage

of the L1 point as a cutoff, and complete three-body dynamics. Simple two-body dynamics overshot the amount of time and fuel mass drastically therefore was not considered a feasible solution. Using the L1 point as a cutoff gave solutions that matched complete three-body dynamics for certain initial conditions; however other initial conditions did not give accurate answers, especially on the moons nearer to Jupiter. Using a percentage of the L1 point yielded good solutions. The problem with this approach was that a different percentage of the L1 point is needed for each situation. No single percentage gives accurate solutions for all the moons. This makes using complete three-body integration necessary to get accurate solutions. A graph was made with trend lines for different thrust-to-weight ratios to allow for the calculations to be made for all possible initial conditions. The transfer time for escaping from or capturing into a moon varies from a couple of days to a month or a month and a half depending on the moon and the thrust-to-weight ratio.

Tangential steering cannot be used in all cases while capturing into or escaping from the moons due to Jupiter's perturbations causing the spacecraft to crash into the moon's surfaces; therefore the new limited-periapsis gain steering law is used to steer the spacecraft. The limited-periapsis gain steering law works by always pointing the thrust in the direction that increases the radius of periapsis the greatest up to the limiter value. The limited-periapsis gain steering law takes virtually the same amount of time to escape as tangent steering if the limiter is set to a small value such as 10 or 20 deg. With these small limiter values the spacecraft never impacts the moon. The greater the value of the limiter, the greater the minimum value of the radius of periapsis is, however the trip time increases.

When the spacecraft is transferring between moons Edelbaum's equation is used. Edelbaum's equation gives comparable values to numerical integration for a spacecraft transferring from one circular orbit to another.

When calculating the entire moon tour, there are two different ranges of power for the engines used. The lower power level engines, 10-20 kW, use a specific impulse of 2700 s and an efficiency of 0.49. The higher power level engines, 50-100 kW, need a greater specific impulse and efficiency however, therefore the value for specific impulse is 7000 s and the efficiency if 0.70. Using the low power thrusters a 1000 kg spacecraft can complete a short mission that would collect small amounts of data in 0.82 yrs travel time with a final mass of 410 kg. Using the high power thrusters a 30000 kg spacecraft can complete a long mission collecting lots of science data in 21.49 yrs with a final mass of 19,906 kg.

The entire Galilean moon tour can be calculated in only minutes with a look up of tables and running a short, efficient MATLAB program. This allows for changes to be made quickly and easily for mission planners that need to know how a change in the mission parameters will affect the trip's results.

REFERENCES

1. http://www.projectrho.com/rocket/Orbits.htm
2. http://www.phy6.org/stargaze/Smotion.htm
3. http://www.spacedaily.com/news/voyager1-03b.html
4. http://www.solarviews.com/eng/jupiter.htm
5. http://nssdc.gsfc.nasa.gov/planetary/lunar/lunargal.html
6. http://nssdc.gsfc.nasa.gov/planetary/galileo.html
7. Sims, Jon A., "Jupiter Icy Moons Orbiter Design Overview," *Spaceflight Mechanics Conference 2006* AAS 06-185
8. Whiffen, Gregory J., and Lam, Try, "The Jupiter Icy Moons Orbiter Reference Trajectory," *Spaceflight Mechanics Conference 2006* AAS 06-186
9. Kowalkoski, Theresa D., Kangas, Julie A., and Parcher, Daniel W., "Jupiter Icy Moons Orbiter Interplanetary Injection Period Analysis" *Spaceflight Mechanics Conference 2006* AAS 06-187
10. Lam, Try, Hirani, Anil N., and Kangas, Julie A., "Characteristics of Transfers to and Captures at Europa," *Spaceflight Mechanics Conference 2006* AAS 06-188
11. Russell, Ryan P., Lam, Try, "Designing Capture Trajectories to Unstable Periodic Orbits Around Europa," *Spaceflight Mechanics Conference 2006* AAS 06-189
12. Thompson, Paul F., Nandi, Sumita, Wong, Mau C., "Orbit Determination Studies for a Low-Altitude Europa Orbiter," *Spaceflight Mechanics Conference 2006* AAS 06-192
13. Paskowitz, Marci E., Scheeres, Daniel J., "A Toolbox For Designing Long Lifetime Orbits About Planetary Spacecrafts: Application to JIMO at Europa," *Spaceflight Mechanics Conference 2006* AAS 06-191
14. Hale, Francis J., *Introduction to Space Flight* New Jersey: Prentice Hall, 1994.

15. Gurzadan, G.A., *Theory of Interplanetary Flights* Australia: Gordon and Breech, 1996.

16. Szebehely, V. G., Theory *of Orbits, the Restricted Problem of Three Bodies*, 1st ed., Academic, New York, 1967, pp. 7-21.

17. Battin, Richard H., *Astronautical Guidance* New York: McGraw-Hill, 1964.

18. http://www.cdeagle.com/ommatlab/crtbp.pdf

19. http://www.hq.nasa.gov/office/pao/History/conghand/propelnt.htm

20. http://nmp.nasa.gov/ds1/gen/gen2.html

21. Kluever, C. A., and Chang, Kun-Rong, "Electric-Propulsion Spacecraft Optimization for Lunar Missions," *AIAA Journal of Spacecraft and Rockets*, Vol. 33, No. 2, 1996, pp.235-239.

22. Kluever, C. A., and Pierson, Bion L., "Vehicle-and-Trajectory Optimization of Nuclear Electric Spacecraft for Lunar Missions," *AIAA Journal of Spacecraft and Rockets*, Vol. 32, No. 1, 1995, pp.126-132.

23. Hack, K.J., George, J. A., and Dudzinski, L.A., "Nuclear Electric Propulsion Mission Performance for Fast Piloted Mars Missions," *AIAA Paper* 91-3488, Sept. 1991.

24. Wilson, John W., "Weight Optimization Methods in Space Radiation Shield Design," *AIAA Journal of Spacecraft and Rockets*, Vol. 12, No. 12, 1975, pp.770-773.

25. Hack, K. J., George, J. A., Riehl, J. P., and Gilland, J. H., "Evolutionary Use of Nuclear Electric Propulsion," *AIAA Paper* 90-3821, Sept. 1990.

26. George, J.A., "Multimegawatt Nuclear Power Systems for Nuclear Electric Propulsion," *AIAA Paper* 91-3607, Sept. 1991.

27. Gao, Y., and Kluever, C.A., "Analytic Orbital Averaging Technique for Computing Tangential-Thrust Trajectories," *AIAA Journal of Guidance, Control, and Dynamics*, Vol. 28, No. 6, 2005, pp. 1320-1323.

28. Battin, Richard H., *An Introduction to the Mathematics and Methods of Astrodynamics* New York: AIAA, 1987.

29. Martini, Mike, "Spacecraft N-Body Analysis Program Users Manual," 2005

30. ftp://naif.jpl.nasa.gov/